ADVANCED MATERIALS
www.advmat.de

Harnessing Extrinsic Dissipation to Enhance the Toughness of Composites and Composite Joints: A State-of-the-Art Review of Recent Advances

Gilles Lubineau, Marco Alfano,* Ran Tao, Ahmed Wagih, Arief Yudhanto, Xiaole Li, Khaled Almuhammadi, Mjed Hashem, Ping Hu, Hassan A. Mahmoud, and Fatih Oz*

Interfaces play a critical role in modern structures, where integrating multiple materials and components is essential to achieve specific functions. Enhancing the mechanical performance of these interfaces, particularly their resistance to delamination, is essential to enable extremely lightweight designs and improve energy efficiency. Improving toughness (or increasing energy dissipation during delamination) has traditionally involved modifying materials to navigate the well-known strength-toughness trade-off. However, a more effective strategy involves promoting non-local or extrinsic energy dissipation. This approach encompasses complex degradation phenomena that extend beyond the crack tip, such as long-range bridging, crack fragmentation, and ligament formation. This work explores this innovative strategy within the arena of laminated structures, with a particular focus on fiber-reinforced polymers. This review highlights the substantial potential for improvement by presenting various strategies, from basic principles to proof-of-concept applications. This approach represents a significant design direction for integrating materials and structures, especially relevant in the emerging era of additive manufacturing. However, it also comes with new challenges in predictive modeling of such mechanisms at the structural scale, and here the latest development in this direction is highlighted. Through this perspective, greater durability and performance in advanced structural applications can be achieved.

1. Introduction

Many advanced materials are not monolithic, and most engineering lightweight structures are assembled from a combination (so-called composite material) of multiple materials. While utilization of composite materials was for a long time limited to very high-performance and low-volume applications, advances in manufacturing technologies, such as resin transfer molding (RTM), out-of-autoclave techniques[1] and additive manufacturing (AM), are improving production efficiency, making composites more competitive for high-volume production.[2] The automotive composites market, for instance, is poised for significant growth, with revenues expected to double by 2032.[3] The rapid adoption of electric vehicles ~~(EVs)~~ further accelerates this trend as the industry shifts toward more sustainable transportation solutions.[4] These new manufacturing paradigms, together with the increasing demand for lightweight vehicles to improve fuel efficiency and reduce emissions, open a new era ofgrowth for nonmetallic materials and their composites.

G. Lubineau, M. Alfano, R. Tao, A. Wagih, A. Yudhanto, X. Li, K. Almuhammadi, M. Hashem, P. Hu, H. A. Mahmoud, F. Oz
Mechanical Engineering Program
Physical Science and Engineering Division
King Abdullah University of Science and Technology (KAUST)
Thuwal 23955-6900, Kingdom of Saudi Arabia
E-mail: gilles.lubineau@kaust.edu.sa; marco.alfano@unimore.it

The ORCID identification number(s) for the author(s) of this article can be found under https://doi.org/10.1002/adma.202407132

DOI: 10.1002/adma.202407132

G. Lubineau, M. Alfano, R. Tao, A. Wagih, A. Yudhanto, X. Li, M. Hashem, P. Hu, H. A. Mahmoud, F. Oz
Mechanics of Composites For Energy and Mobility Lab
King Abdullah University of Science and Technology (KAUST)
Thuwal 23955-6900, Kingdom of Saudi Arabia

M. Alfano
Dipartimento di Scienze e Metodi dell'Ingegneria, Universita' degli Studi di Modena e Reggio Emilia
Reggio Emilia (RE) 42122, Italy

R. Tao
Aerospace Structures & Materials
Faculty of Aerospace Engineering
Delft University of Technology
Kluyverweg 3, Delft 2629 HS, The Netherlands

A. Yudhanto
Department of Mechanical Engineering
Baylor University
Waco, TX 76798, USA

Mechanical interfaces are crucial for developing reliable composite-based lightweight solutions (see **Figure 1a**). It involves the joining of separately manufactured parts with maximum efficiency and minimal weight to maintain the competitive advantage of fiber-reinforced polymers (FRPs). In sectors such as mobility (automotive, rail, aeronautics, aerospace) and renewable energy, achieving net-zero CO_2 emissions increasingly depends on the effective joining of FRPs with other FRPs or metallic parts, where minimal weight and maximum performance are paramount.[5] The renewable energy sector, for example, relies heavily on multi-interface materials to fabricate high-performance wind turbine blades, demonstrating the critical role of mechanical interfaces in advancing sustainable technologies. Therefore, interfaces play a pivotal role in both composite materials and their joints, as they are essential for ensuring structural integrity and performance across a range of applications. The effectiveness of these interfaces directly influences the overall functionality and durability of the engineered components. For example, carbon fiber-reinforced polymers (CFRPs) have long been the material of choice for lightweight shells, including aircraft fuselages and are renowned for their excellent in-plane properties. However, CFRPs exhibit weak out-of-plane properties and, as shown in Figure 1a, they are subjected to service-related damage and/or cracks. Since their through-thickness performance depends solely on the properties of the resins (thermoset or thermoplastic), CFRPs are prone to delamination, i.e., the separation between the plies, especially when brittle thermoset resins are used as matrix material. This issue is well known: barely visible damage has been a persistent challenge for composite designers, as low-energy impacts on CFRPs can cause extensive delamination within the laminated structure with little to no surface evidence.

It follows that the engineering community has developed various solutions to mitigate sensitivity to delamination. For example, recent studies have shown that incorporating toughened resin systems into the matrix can enhance crack propagation resistance and reduce delamination risk. Adding thin layers of tougher materials, such as thermoplastic films or interleaved layers, between composite layers can act as barriers to crack progression.[6,7] Additionally, introducing vertical fibers, known as "Z-pins," or mechanically stitching layers together can strengthen interlaminar bonds and decrease the likelihood of delamination.[8] While these techniques can significantly improve out-of-plane properties, they may reduce in-plane properties due to the resulting in-plane waviness of the microstructure.

Strategic design and manufacturing choices, such as optimal ply orientation, can minimize the risk of delamination and leverage its effects to counteract crack propagation.[9] However, this approach is limited by the complexity and cost of achieving precise ply angles, which may not always be feasible in all manufacturing settings. Furthermore, nano-engineered interfacial layers, such as those incorporating carbon nanotubes (CNTs), can significantly enhance interlaminar strength and toughness.[10–12] Nonetheless, these advanced materials often come with drawbacks, including high production costs, difficulties in uniform dispersion within the matrix, and potential challenges in maintaining long-term performance due to possible degradation of the nanomaterials over time.

Additional concerns arise with joining of composites. Traditional joining technologies, such as fastening with rivets or bolts, present several drawbacks, including stress concentration in substrates, significant weight increase due to fastening elements, additional machining steps that incur extra costs, and compromised lifecycle of the structure due to the need for maintenance and repairs.[13] As an alternative, engineers are turning to adhesive bonding, where the mechanical interface relies solely on an additional adhesive layer without mechanical fasteners.[14] Although adhesive bonding is theoretically attractive, its performance is highly sensitive to adherent surface preparation, which can be mechanical or chemical.[15] While chemical treatments are generally more effective, providing better cleaning and functionalization of surfaces, they also generate large volumes of chemical waste and pose health, safety, and regulatory concerns. Therefore, there is a clear need for new technologies that improve the performance of secondary bonded structures beyond the current techniques available in the industry.

Based on the above discussion from the structural and material side, it becomes evident that new solutions are needed for creating mechanically high-performance interfaces without compromising the substrates' integrity. These new solutions should improve basic metrics such as interface strength and fracture toughness and enhance safety by preventing unstable and uncontrolled delamination, which can result in loss of structural integrity with no opportunity for maintenance and repair.

Examining how energy is dissipated, both locally at the material level and non-locally during crack propagation, can provide the foundation for creating more robust interfaces that improve strength and fracture toughness while ensuring the structural integrity and safety of composites and composite joints. Energy dissipation during delamination always results from the superposition of two contributions: (1) *intrinsic* local dissipation, which can be considered a material property and corresponds to the work of separation needed at the material point level, and (2) *extrinsic* non-local dissipation, which arises from the dissipation in the volume associated with crack propagation (including regions away from the crack path). These contributions are illustrated in the schematic of Figure 1b, which provides representative examples for each of the intrinsic and extrinsic sources of dissipation mentioned above. For example, in composite laminates, intrinsic dissipation describes mechanisms that depend on the inherent properties of the constituents of the composite material, such as fiber breakage, matrix micro-cracking, and fiber-matrix debonding. These internal damage mechanisms absorb energy as the composite undergoes deformation or fracture.[16] On the other hand, extrinsic dissipation describes long-range mechanisms that can take various forms, ranging from plasticity and

K. Almuhammadi
Novel Nonmetallic Solutions
Dammam 33228, Kingdom of Saudi Arabia
M. Hashem
NEOM
Design and Construction Sector
Tabuk 49643, Kingdom of Saudi Arabia
P. Hu
Department of Mechanics and Engineering
Aarhus University
Aarhus 8200, Denmark

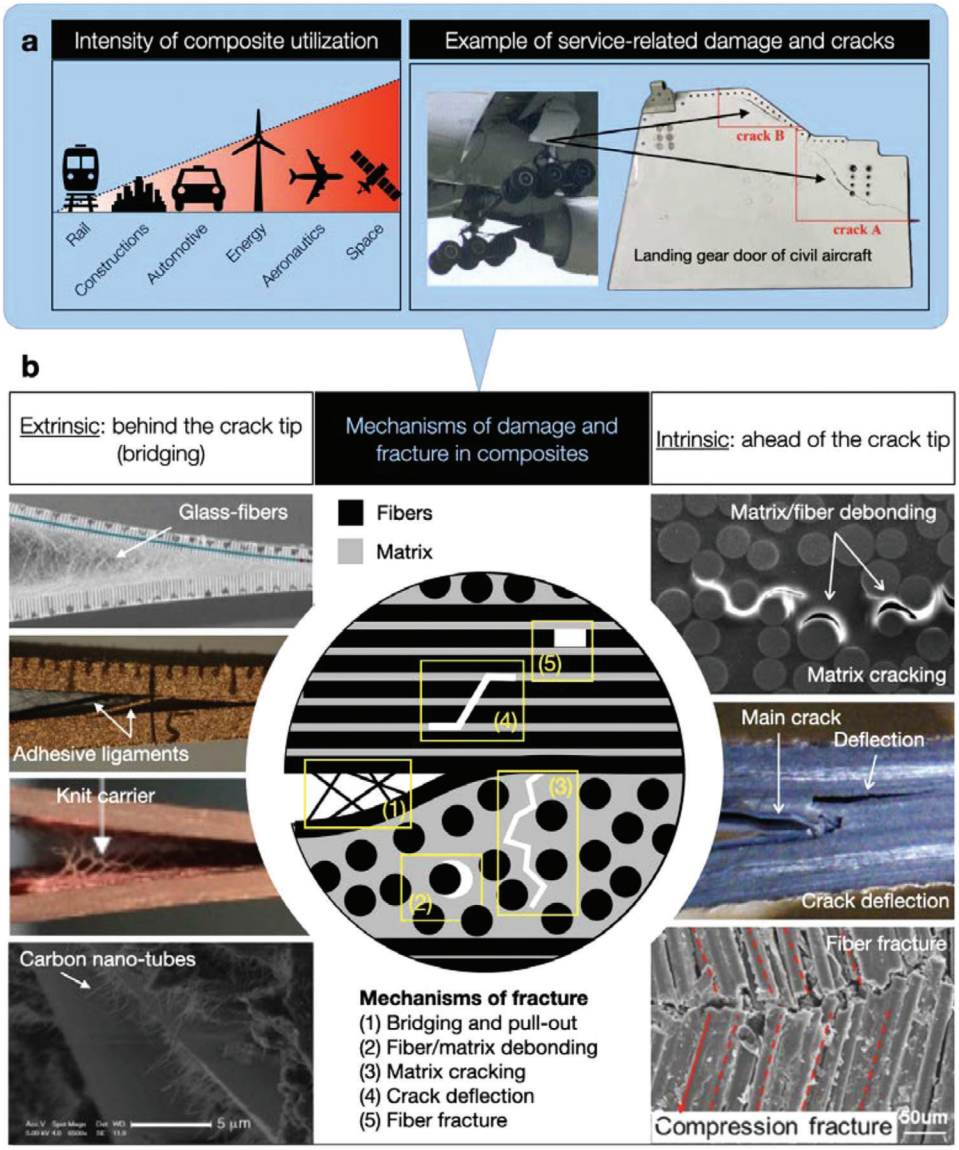

Figure 1. a) Intensity of composite material utilization in the most common industries and an example of service-related damage and cracks. Reproduced with permission.[26] Copyright 2024, Elsevier B.V. b) Mechanisms of damage and fracture in laminated structures, from top-left corner (in counterclockwise direction): fiber bridging in glass-fiber reinforced composites (GFRP) (Reproduced with permission.[27] Copyright 2014, Elsevier B.V.); adhesive ligament bridging in bonded CFRP (Reproduced with permission.[14] Copyright 2018, Elsevier B.V.); bridging of a knit carrier in CFRP substrates bonded with an adhesive film (Reproduced with permission.[28] Copyright 2018, Elsevier B.V.); bridging of CNTs (Reproduced with permission.[11] Copyright 2010, Elsevier B.V.); fiber fracture (Reproduced with permission.[29] Copyright 2023, Elsevier B.V.); crack deflection (Reproduced with permission.[30] Copyright 2023, Elsevier); matrix cracking and matrix/fiber debonding (Reproduced with permission.[31] Copyright 2012, Elsevier B.V.).

fragmentation in the process zone to large-scale bridging, which is an exceptionally efficient toughening mechanism.

Extrinsic dissipation involves mechanisms that shield the crack tip from mechanical stresses, thereby reducing crack propagation. In FRPs, examples of extrinsic dissipation include fiber pull-out, bridging, and crack deflection.[17] Fiber pull-out occurs when fibers are pulled out of the matrix as the composite fractures, absorbing energy in the process.[18] Bridging involves fibers that span the crack, holding the fracture faces together and absorbing energy as the crack opens.[19,20] Crack deflection occurs when the crack path changes its direction due to the composite's inherent microstructure, increasing the fracture's surface area and enhancing energy absorption.[21,22] While extrinsic dissipation mechanisms are often complex due to their dependence on the structure kinematics and the intricate interactions within the material, they offer significant advantages in improving the toughness and durability of FRPs. Understanding and utilizing these mechanisms can be challenging, but their ability to enhance fracture resistance makes the effort worthwhile.

This enhancement is typically reflected in a rising R-curve, a desirable trait in many engineering applications. Non-local mechanisms, such as fiber bridging, exemplify this potential.

Fiber bridging becomes increasingly active as cracks propagate, providing additional resistance against crack growth. Therefore, short cracks may only exhibit toughness comparable to the intrinsic part, but as the crack grows, the extrinsic dissipation due to bridging comes into play, markedly increasing toughness. The combined effect of intrinsic and growing non-intrinsic contributions can substantially improve the structural integrity and durability of composite materials and adhesive bonds.

Despite the challenges in describing and implementing extrinsic dissipation in engineering structures, its potential to significantly enhance performance makes it an invaluable tool in designing advanced materials and structures. For this reason, over the past ten years, our team has strategically focused on optimizing extrinsic dissipation, especially in the context of laminated composites—see for instance,[14,19[23–25]] to list a few. This concerted effort culminated in developing various technologies that, while differing in their implementation, requirements, and performance, all aim to modify the effective toughness through a deep understanding of intrinsic-extrinsic partition of the dissipated energy.

The aim of this paper is to review cutting-edge technologies developed in this field by the present authors and others. Our objective is to offer specific insights into interfacial fracture and delamination, particularly in contexts where energy dissipation is governed by extrinsic mechanisms, such as bridging away from the crack tip and structural modifications away from the crack path. We have concentrated on the key studies that effectively convey these ideas in the context of composites and their joints, while also considering the emerging potential of additive manufacturing in this field.

Following the current introduction, a second section is dedicated to classical delamination in laminated structures and its description. Therefore, the degradation mechanisms and their mathematical description in this section are considered intrinsic. Section 3 outlines the limitations of these approaches by highlighting evidences of the importance of extrinsic features in the observed effective dissipation. Extrinsic effects are discussed in many structures, ranging from nano-reinforced composites to continuous fiber composites. Section 4 illustrates how such extrinsic dissipation can be used to improve the performance of the structure, especially its effective toughness. Section 5 focuses on the modeling challenges, as very few computational approaches today account for a physics-based description of the extrinsic effect, despite its potential to drastically modify the predicted result. Section 6 finally focuses on applications and demonstrates how interfaces based on these new concepts can greatly outperform classical designs. This structured approach not only provides a comprehensive understanding of both intrinsic and extrinsic dissipation mechanisms but also offers practical insights into how these concepts can be effectively applied to advance the design and performance of composite structures.

2. Classical Approaches to Delamination in Laminated Structures

2.1. Experimental Observations

Delamination is a critical fracture mechanism in composite laminates.[32] This failure mode, often due to fiber-matrix debonding or matrix cracking as illustrated in **Figure 2**a, significantly weakens structural integrity by reducing stiffness and strength, limiting load-bearing capacity. Localized delaminations create stress concentrations that can propagate further damage,[33] interrupt uniform stress distribution, and make composites more vulnerable to failure under load. This process also negatively impacts the in-plane strength of a composite.[32] High interlaminar stresses and the low through-thickness strength of laminates cause delamination.[34] Since fibers do not offer reinforcement in the through-thickness direction, the composite relies on the weaker matrix for load-bearing capacity, exacerbated by the brittle nature of matrix resins.[35] Shear and tensile stresses from out-of-plane loading or impacts (e.g., bird strikes, hail) can cause sudden delamination or matrix cracking, breaking through the interface between plies.[33] These stresses can result from external loading, structural geometry, and localized flaws and cracks.[36]

The stacking sequence of a composite panel is crucial in determining the delamination path, which can vary from smooth to stair-shaped profiles, as shown in Figure 2b.[37] To increase fracture toughness compared to a straight delamination front, attempts have been made to engineer the crack path, illustrated in Figure 2c.[21] Additionally, delamination in laminates with bending-twisting (BT) coupling may cause occasional fiber bundle bridging, releasing energy upon rupture. Conversely, a stacking sequence resulting in bending-extension (BE) coupling can induce a stress field characterized by mode II shearing, enhancing toughness through matrix shear failure.[38] Figure 2d shows the fracture surfaces in such scenarios.

Delamination is also promoted by local changes in thickness or curved boundaries in composite components, causing high shear and normal stresses at the interface.[39] Even higher localized stresses arise from flaws and cracks that can be generated during manufacturing (e.g., machining damage or imperfections),[40,41] during service,[42] or from the presence of cut and discontinuous plies within the layup.[43] Additional sources of discontinuities include the free edges of the laminate due to differences in the Poisson ratio between adjacent plies with different orientations.[44]

Delamination in composites can be studied using several mechanical testing methods. The most common methods are shown in **Figure 3**. These tests promote the delamination process under controlled conditions to assess the interlaminar properties and delamination resistance of composite materials. Common methods include Mode I delamination testing using the Double Cantilever Beam (DCB), which measures interlaminar fracture toughness in Mode I (G_{Ic}).[45] Mode II testing uses the End Notched Flexure (ENF) test, which evaluates interlaminar fracture toughness in Mode II (G_{IIc}) by bending the specimen to induce crack propagation from a pre-existing starter crack.[46] Recently, by tuning the geometry of specimen cross section, the issue of instability for the classical ENF has been effectively addressed.[47] Delamination testing can also be accomplished using the Edge Crack Torsion (ECT) test, which measures interlaminar fracture toughness in Mode III (tearing mode).[48] The specimen is twisted to create a crack at a pre-existing notch, and the mode III critical energy release rate is calculated. The resistance to crack propagation under combined loading of the crack faces is also important. Mixed-Mode testing is conducted

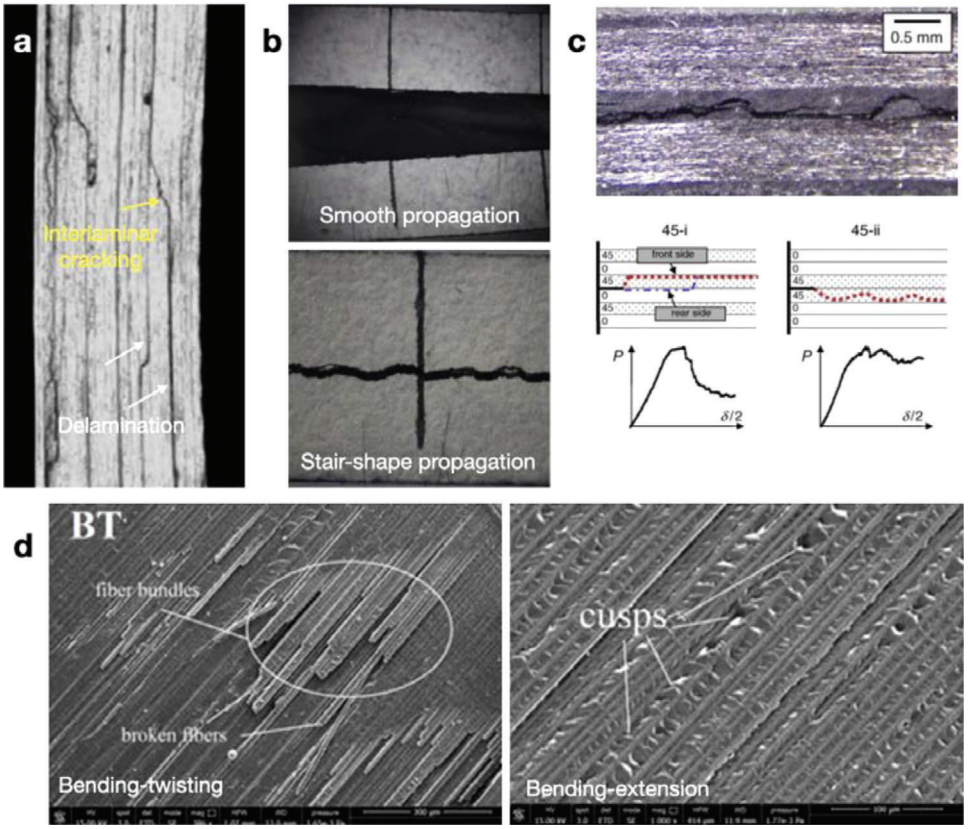

Figure 2. a) The combined action of shear and tensile stresses due to out-of-plane loading can cause sudden delamination or matrix cracking that breaks through the interface between plies. Reproduced with permission.[33] Copyright 2024, Elsevier B.V. b) Delamination path depends on the stacking sequence and can vary from smooth to stair-shaped profiles. Reproduced with permission.[37] Copyright 2012, Elsevier B.V. c) The crack path can be engineered to control crack growth and increase toughness compared to a straight delamination front. Reproduced with permission.[21] Copyright 2014, Elsevier B.V. d) Delamination at the interlaminar interface in a laminate with BT coupling may exhibit occasional fiber bundle bridging that releases energy upon breaking. A stacking sequence leading to BE coupling can cause a stress field dominated by mode II shearing of the crack faces, increasing toughness due to shear failure of the matrix. Reproduced under the terms of the CC-BY Creative Commons Attribution 4.0 International license (https://creativecommons.org/licenses/by/4.0).[38] Copyright 2020, The Authors, published by MDPI(Multidisciplinary Digital Publishing Institute).

using the Mixed-Mode Bending apparatus (MMB) to assess interlaminar fracture toughness under combined opening and shear loading.[49] The mix ratio between Modes I and II can be varied by adjusting the lever arm, and the critical energy release rate (G_c) is calculated. Furthermore, the above tests are often adapted to fatigue testing, which involves cyclic loading of a composite specimen to study how delamination progresses. These tests provide insights into the growth rate of delamination and the composite's resistance to fatigue-induced damage.

Special attention must be paid when post-processing experimental data from such tests, particularly in cases where extensive extrinsic dissipation occurs. Traditional post-treatment techniques, which rely on fracture mechanics assumptions and simplistic beam theories, are primarily tailored for scenarios dominated by intrinsic dissipation. By employing the mitigation strategies outlined in this review, it becomes feasible to capitalize on advantageous extrinsic sources of energy dissipation, such as fiber bridging. These mechanisms exhibit strong non-local effects and consequently alter the interfacial kinematics.[22,27,50–55] Consequently, the calculation of the energy release rate (ERR) deviates from classical equations presented in standards,[45,46,49] necessitating the application of concepts such as the J-integral.[56]

2.2. Modeling Approaches

Various modeling techniques, mostly within the finite element method (FEM) framework, have been devised to simulate the fracture and failure responses of composites. These techniques are broadly classified into two families: Smeared Continuum Damage Models (SCDM)[57,58] and Discrete Crack Models (DCM).[59,60] Most models today do not properly account for extrinsic dissipation, lumping it into the intrinsic part.

SCDM smears fractures into a finite element band of homogeneous continua, characterized by internal state variables dependent on stress and energy dissipation.[61–64] However, SCDM suffers from mesh dependence issues.[58,65]

Recently, phase field methods (PFM) have gained attention as a non-local version of SCDM. PFM uses a partial differential equation for an auxiliary field (phase field) to represent fracture.[66–68] This method minimizes the total potential energy of the system, eliminating the need for specific crack nucleation criteria.[69] SCDM does not require prior knowledge of crack paths but faces challenges with crack nucleation and other ill-posed issues.

SCDM has been used for predicting intralaminar failure and delamination.[64,70–77] However, DCM is favored for explicit crack

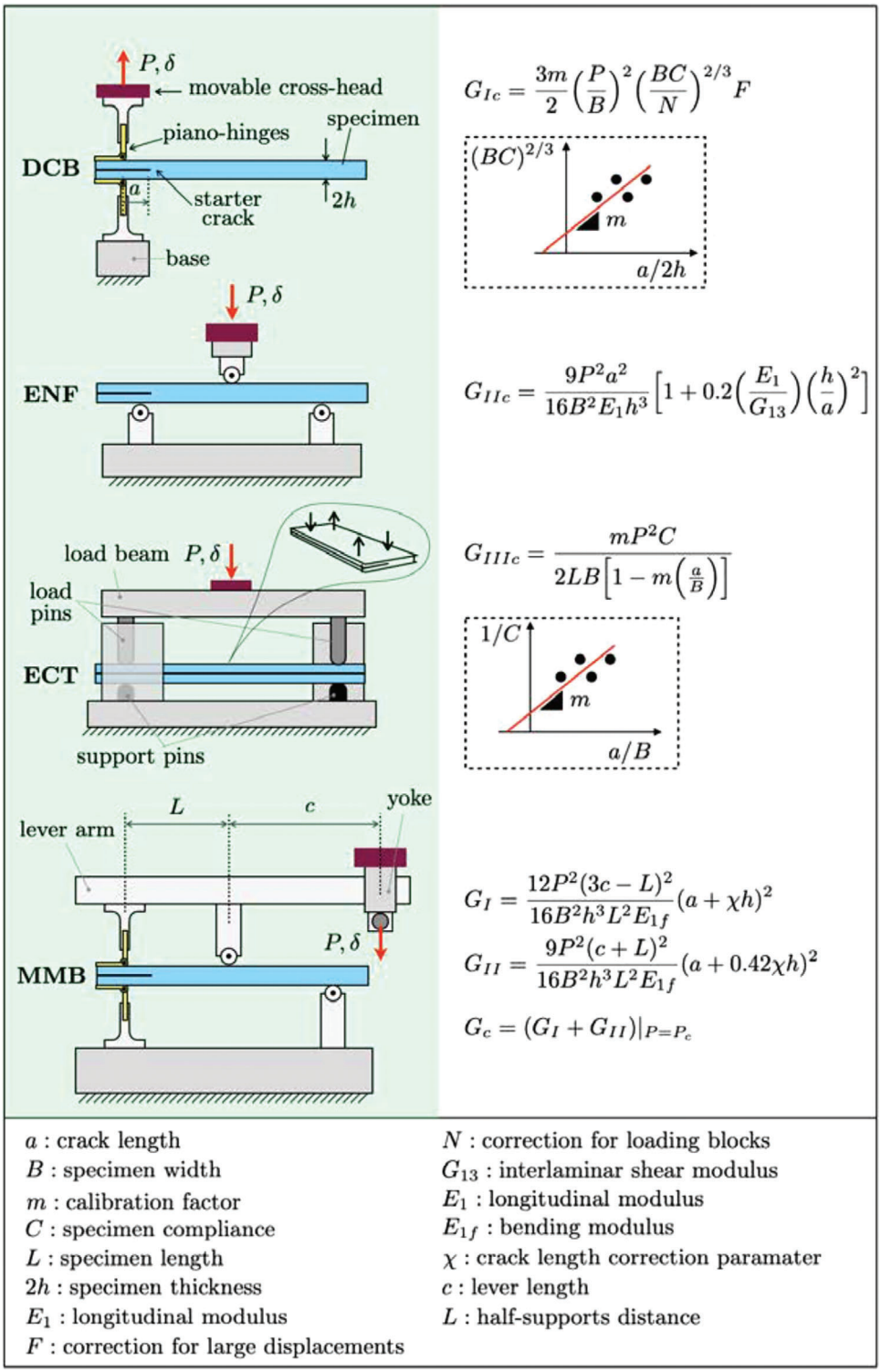

Figure 3. Most common test specimens adopted for delamination testing of polymer-based composites. DCB; ENF; ECT; MMB.

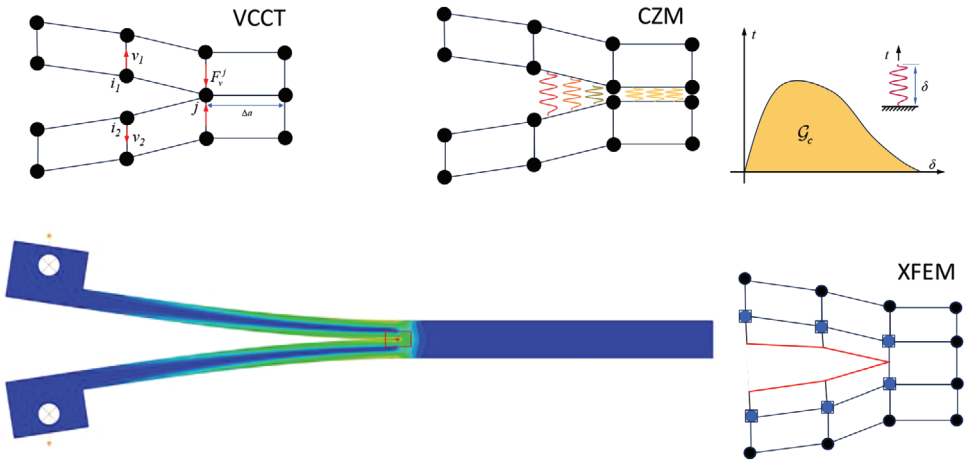

Figure 4. Schematic of different numerical approaches for modeling Mode I fracture.

tracking, simpler numerical treatments, and alignment with fracture mechanics theories, though it often requires prior knowledge of the crack path, suitable for delamination and interfacial fractures.

2.2.1. Virtual Crack Closure Technique (VCCT)

The VCCT is rooted in the theoretical framework of linear elastic fracture mechanics (LEFM), assuming that when a crack is extended, the ERR is the same required to close it.[78] In VCCT, the crack front is discretized into finite elements, and the displacement jumps across the crack are assumed to be self-similar and closed by applying virtual forces. A comprehensive review of the history of VCCT has been made by Krueger.[79]

As illustrated by **Figure 4**, assuming a linear nodal force variation during closure and a self-similar delamination growth, the energy to close the crack (and, thus, the ERR) is calculated and compared to the critical ERR using:

$$f = \frac{\mathcal{G}_I}{\mathcal{G}_{IC}} = \frac{1}{2b\Delta a}\left(\left|v_1^i - v_2^i\right|F_v^j\right)\frac{1}{\mathcal{G}_{IC}} \geq 1.0 \tag{1}$$

where $\mathcal{G}_I$ is the Mode I energy release rate, $\mathcal{G}_{IC}$ is the critical Mode I ERR, b is the width of element, Δa is the length of the elements at the crack front, F_v^j is the vertical force between nodes j_1 and j_2, and $\left|v_1^i - v_2^i\right|$ is the vertical relative displacement between nodes i_1 and i_2. Similar arguments and equations can be written in two dimensions for Mode II and 3D crack surfaces, including Mode III. Furthermore, VCCT can account for mixed-mode loading by considering the contributions of various mode components to the overall ERR, thereby enhancing its predictive capacity. In mixed mode condition, the equivalent ERR $\mathcal{G}_{\text{equiv}}$ is computed and compared to $\mathcal{G}_{\text{equivC}}$, the equivalent critical ERR subjected to a specific mode mixity. The crack propagates when:

$$f = \frac{\mathcal{G}_{\text{equiv}}}{\mathcal{G}_{\text{equivC}}} \geq 1.0 \tag{2}$$

This calculation can be done based on the user-specified mode-mix laws. Three common mode-mix formulae are adopted as the criterion for characterizing the crack propagation subjected mixed mode loads, i.e., the Benzeggagh–Kenane law,[80] the power law,[81] and the Reeder's law.[82] The choice of mixed mode propagation law is not always clear in any given analysis; an appropriate law is best selected empirically. Overall, VCCT's theoretical foundation in fracture mechanics allows for robust and accurate analysis of delamination behavior, making it an indispensable tool in studying composite materials.

Nevertheless, VCCT demands meticulous modeling of the crack front and judicious mesh refinement while facing challenges in accurately capturing mixed-mode delamination phenomena.[83] More importantly, VCCT can only characterize the self-similar brittle and cleavage fracture process, which makes it inaccurate when modeling delamination processes with extrinsic dissipation events subjected to complicated loading conditions. Despite these constraints, VCCT remains indispensable in industries for delamination analysis because only the critical energy release rate (G_c) is needed in the modeling.

2.2.2. Cohesive Zone Model (CZM)

The CZM, rooted in Dugdale and Barenblatt's work[84,85] and further developed by,[86] is a robust DCM technique used in composite laminates, bonded joints, and adhesive interfaces to predict debonding and delamination under a variety of loading conditions.[87–90] CZM, using cohesive laws to characterize traction-separation (TS) behavior, simulates delamination by incrementally opening cohesive zones[91] and is implemented in FEM codes like ABAQUS.[92,93] Unlike VCCT, CZM handles both fracture initiation and propagation, requiring extensive parameter calibration.[94,95] It predicts non-self-similar delamination growth, evolving throughout the loading history, and can be combined with plasticity models to capture ductile fracture behavior.[96,97] The TS law can be generally expressed by the following:

$$t = K(1-d)\delta \tag{3}$$

where K is the initial stiffness, normally set to a large value to characterize the integrity of intact interfaces and avoid

compressive penetration; d is the degradation scalar, and t and δ are the traction and separation of the interface, respectively. Note that multiple scalar damage measures can be used in different loading directions in case of non-isotropic degradation.

The onset of delamination is generally determined by some criterion in terms of stress or strain, and the propagation is characterized by the same criterion by Equation (2). The power and Benzeggagh–Kenane laws are applied when dealing with mixed mode propagation in CZM.[98]

CZM's physically-based approach offers versatility in modeling mixed-mode delamination and accommodating a wide range of material properties and loading scenarios, providing detailed insights into the mechanisms governing delamination growth.[99] However, CZM does present challenges, particularly in terms of parameter calibration, where cohesive zone parameters such as cohesive strength and fracture energy must be accurately determined and the TS responses may vary with material properties, loading rates, orientation and even the geometrical pattern of the interface fracture of composites[56,100,101] and others, such as biological interfaces.[102,103] The identification of TS laws primarily relies on advanced local deformation measurements and advanced modeling approaches.[91,104–108] And characterizing such complexity by using CZM is still problematic. Despite these limitations, CZM remains the most applied technique when modeling the delamination behavior, which could significantly aid in engineering design and optimization efforts across diverse industries.

Ongoing research is crucial to addressing these challenges and further enhancing the applicability of CZM to complex delamination scenarios in practical engineering applications. In particular, once the fracture toughness values for each mode are determined, they are assumed to remain constant throughout the delamination process. While this assumption simplifies calculations, it overlooks potential variations due to factors such as fracture direction or evolving delamination kinematics. Moreover, the constant fracture toughness assumption fails to capture nonlocal effects like fiber bridging. This leads to imprecise quantification of fracture toughness in laminates and inaccurate predictions of delamination responses in FRP composites. For more details about how to apply the CZM-based elements, including the determination of element size and parameters, readers can refer to Refs. [109–111].

2.2.3. Extended Finite Element Method (XFEM)

Both VCCT and CZM require setting the crack propagation *a priori*. To address this limitation, adaptive re-meshing techniques for crack growth have been developed.[112] However, the low computational efficiency impedes its broad applications of re-meshing approaches, except for very specific situations using a very well-optimized mesh data structure. The XFEM, as a particular instance of the DDMs, offers a sophisticated solution to model crack propagation without the need for either a prior crack path or re-meshing,[113,114] cf. [115] for a similar approach applied for delamination modeling.

Based on the partition of unity concept, XFEM enriches the traditional finite element approximation space with additional degrees of freedom to represent cracks and delaminations (as schematically shown in Figure 4), allowing for an accurate depiction of complex crack geometries and interactions.[114,116] Its applications encompass a wide range of scenarios, including composite laminates,[116–118] bonded joints,[119] and structures subjected to various loading conditions. XFEM has also been coupled with other DDM approaches, such as CZM[120,121] and VCCT,[122] and even SCDM-type models,[123] to model complex failure mechanisms of composites.

Despite its advantages, XFEM poses challenges, particularly in the careful selection of enrichment functions and integration techniques to ensure accurate representation of discontinuities.[124,125] This may increase computational cost and complexity, resulting in convergence issues. Additionally, XFEM may encounter difficulties capturing crack-tip singularities and sharp corners, especially in heterogeneous materials or complex loading conditions. Further research must address its limitations and enhance its applicability to complex delamination scenarios in practical engineering applications.

A thorough analysis comparing the efficacy of VCCT, CZM, and XFEM in modeling 2D and 3D delamination is undertaken, assessing their performance in simulating the delamination process of a DCB sample.[83,126] It should be mentioned that while classical DCM approaches may yield satisfactory results for simple/cleavage-type delamination fronts, they often struggle to address the delamination scenarios where multiple non-local failure mechanisms across various length scales are presented.

Based on this brief overview of classical delamination results and associated numerical techniques, it appears that the design, modeling, and simulation of delamination mechanics using non-local/extrinsic dissipation is still largely to be developed. The remaining document presents experimental evidence of extrinsic dissipation, technologies inspired by these observations, and new modeling approaches to push forward predictive simulations in this context.

3. Extrinsic Dissipation Mechanisms in Laminated Structures

Among all extrinsic mechanisms taking place in laminated composites, crack bridging is probably the biggest source of dissipation.[19] By spanning cracks with fibers or particles, the crack faces are held together, which helps distribute stress around the crack tip and slow down crack propagation. This process maintains the structural integrity of the composite by delaying further crack growth. Bridging occurs across multiple scales, from nanoscale to macroscale, providing various opportunities for improving the fracture resistance and mechanical properties of composite laminates. At the nanoscale, bridging involves using nanoparticles, such as CNTs, within the matrix.[127] These nanoparticles can span across cracks at a very fine scale, contributing to crack arrest and improving the mechanical properties of the matrix.[128] At the microscale, chopped fibers dispersed within the matrix form the basis of microscale bridging. These shorter bridging fibers help absorb energy during crack propagation, enhancing the composite's overall toughness.[129] Finally, at the macroscale, long fibers, either continuous or in bundles, can bridge cracks within the composite structure. When cracks open, these long fibers remain intact across the crack, exerting tension and absorbing energy.[20,22]

Table 1. Summary of key carbon-based fillers at nano, micro, and macro scales and their contributions to energy dissipation.

Scale	Toughening/Reinforcement Method	Advantages	Level of Enhancement
Nanoscale			
Nano	Carbon Nanotubes (CNTs)	✓ High mechanical strength and low density. ✓ Enhanced interfacial bonding due to high aspect ratio. ✓ Effective (small-scale) crack bridging and load transfer. ✓ Enhanced energy dissipation through CNT-enabled frictional sliding and void growth.	• Up to 50% increase in interlaminar fracture toughness (He et al. [130]). • Reduced delamination rates (Grimmer et al. [128]). • Improved durability under cyclic loading (Lubineau et al. [127]).
Nano	Carbon Nanofibers (CNFs)	✓ Effective (small-scale) crack bridging. ✓ Enhanced pull-out and frictional sliding mechanisms for greater energy dissipation. ✓ Improve energy dissipation during fracture. ✓ CNFs enabled void-growth.	• Up to 30% increase in mode I initiation toughness (Ladani et al. [131]). • Enhanced fracture toughness (Ravindran et al. [132]).
Microscale			
Micro	Short Carbon Fibers (SCFs)	✓ Energy absorption during crack propagation. ✓ Improved toughness through intrinsic and extrinsic mechanisms. ✓ Enhanced interfacial shear strength. ✓ Promote pull-out mechanisms for energy dissipation.	• Increased mode I fracture toughness (Ravindran et al. [129]). • Up to 30% increase in impact resistance (Ravindran et al. [132]).
Macroscale			
Macro	Long Fibers (e.g., Continuous Carbon Fibers) and their bundles	✓ Significant load-bearing capacity. ✓ Effective in bridging cracks. ✓ Improved resistance to crack propagation.	• Enhanced propagation toughness (Farmand et al. [50]). • Improved delamination resistance ([133, 134]).

In the subsequent sections, we will examine bridging at the nano, micro, and macro scales more in-depth. We will explore the different types of fibers and particles used in bridging, how these materials interact with cracks at each scale, and the various techniques used to enhance the mechanical properties of composite laminates through bridging.

Table 1 summarizes key fillers used to trigger bridging, specifically focusing on carbon nanotubes (CNTs), short carbon fibers (SCFs), and carbon nanofibers (CNFs). These methods are evaluated based on their unique advantages and the levels of enhancement they provide in terms of fracture toughness and damage resistance (**Figure 5**). For instance, CNTs offer significant improvements in interlaminar fracture toughness and durability due to their high mechanical strength and effective crack bridging capabilities. On the other hand, SCFs contribute to energy absorption during crack propagation, while CNFs enhance both toughness and energy dissipation through their unique structural properties. The insights provided in the table highlight the potential of these materials in advancing composite performance in various applications.

3.1. Nano- and Micro-Scale Bridging Mechanisms

Recently, integrating CNTs into CFRP composites to create a multi-scale or hierarchical structure has emerged as an effective approach to significantly enhance the interfacial fracture toughness while maintaining in-plane mechanical properties. The improvement is largely attributed to CNTs' nanoscale size and exceptional mechanical properties, including an elastic modulus of approximately 1 TPa and tensile strength of around 100 GPa.[127] Typically, there are three main methods for incorporating CNTs into composites: mixing them with resin,[7,128–132]

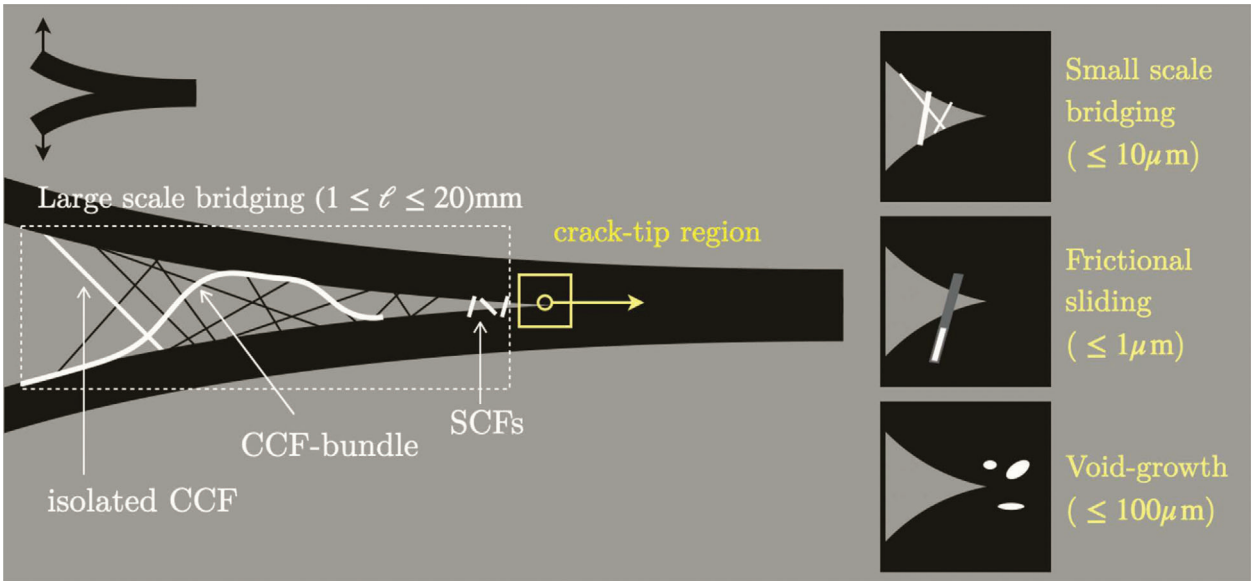

Figure 5. Bridging mechanisms spanning over various scales, depending on the type of reinforcement: CNTs or CNTs will introduce nanoscale bridging, while SCFs will influence the micro scale and CCFs can introduce long-range bridging.

in situ growth or grafting onto fibers,[135] and inserting macroscopic CNT assemblies.[12,136]

The enhancement of mechanical properties can be understood through several mechanisms. Incorporating CNTs can improve the mechanical properties of the polymer matrix within the composite laminate. When dispersed evenly throughout the matrix, CNTs (*i*) act as reinforcement, absorbing and redistributing stress more effectively throughout the material while constraining the polymeric chains; (*ii*) improve the bond between the fibers and the matrix, leading to significant improvements in the interfacial strength as they facilitate a more effective transfer of stress from the matrix to the fibers; (*iii*) enhance the toughness of the composite by promoting fragmentation and pull-out based dissipation. There is extensive evidence that CNTs can help bridge cracks and prevent crack propagation, contributing to greater overall durability and resistance to failure.[127]

Grimmer et al.[128] showed that mixing small amounts of multi-walled CNTs to the matrix of glass-fiber composites significantly reduced delamination crack propagation rates and increased interlaminar fracture toughness. Scanning electron microscopy revealed that CNTs at the delamination crack front slowed down crack propagation through CNTs bridging, followed by their pull-out and fracture. This shift in fracture behavior enhanced interlaminar fracture resistance compared to composites without CNTs. He et al.[130] presented a toughening strategy using hierarchical architecture, where CNTs are stitched between carbon fibers at the interlaminar region using a multi-layer resin film infusion process. The results of Mode I fracture tests, which are reported in **Figure 6a**, indicated that even a low concentration of CNTs (0.3 wt%) led to a 50% increase in mode I fracture energy G_{Ic}, from 1.099 to 1.648 N mm^{-1}. Likewise, the figure shows that the improved toughness resulted from the hierarchical architecture combining CNT nano-bridging with carbon fiber bridging, as observed by scanning electron microscopy (SEM) analysis.

Ravindran et al.[129,132] and Ladani et al.[131] investigated multiscale toughening mechanisms in CFRPs to enhance interlaminar fracture toughness, low-velocity impact damage resistance, and compression-after-impact (CAI) strength. They used carbon nanofibers (CNFs) and short carbon fibers (SCFs) in the epoxy matrix, both separately and in tandem. Fractographic analysis of DCB test specimens revealed that CNFs and SCFs, when used individually, increased mode I initiation and steady-state fracture toughness. Ahead of the crack tip, CNFs and SCFs facilitated intrinsic toughening through interfacial debonding and plastic void growth. Behind the crack tip, extrinsic toughening included pull-out, bridging, and rupture of CNFs and SCFs. SEM analyses showed a polymer-rich layer (30–50 μm) between carbon fabric layers, with longer SCFs (approximately 710 μm) aligning parallel to the ply layers. The results of mode I fracture toughness, along with the mechanisms of extrinsic dissipation (before and after the addition of nano-reinforcement), are exemplified in Figure 6b.

Ou et al.[7] demonstrated that the effectiveness of crack bridging by dispersed CNTs depends heavily on the average length of the dispersed phase. The authors incorporated short CNT powders (average length < 1μm) into the epoxy matrix of unidirectional CFRP composites to enhance toughness and achieve uniform dispersion between carbon fibers. The findings revealed that 0.5 wt% was the optimal loading level of CNT powders for matrix toughening, with a notable increase of 62% in Mode I interlaminar toughness at the crack initiation phase, which the authors attributed to the improved mechanical properties of the matrix. However, the shorter average length of CNT powders resulted in minimal contribution during the crack propagation phase, leading to a relatively flat R-curve and limited evidence of bridging.

Using CNTs to enhance toughness in composites faces several challenges. The effectiveness of crack bridging by CNTs largely depends on their average length, with shorter CNTs (e.g., < 1μm) contributing minimally during the crack propagation

Mixing of CNTs within composites matrix

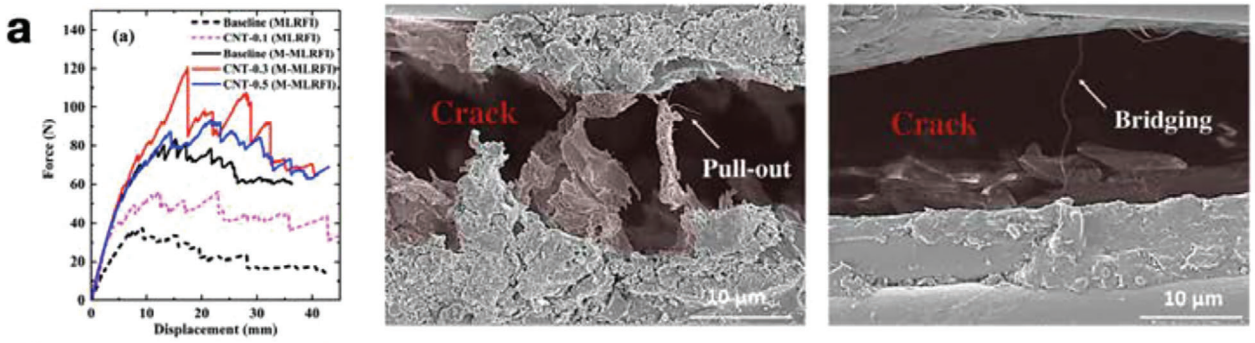

Mixing of nano fibers within composites matrix

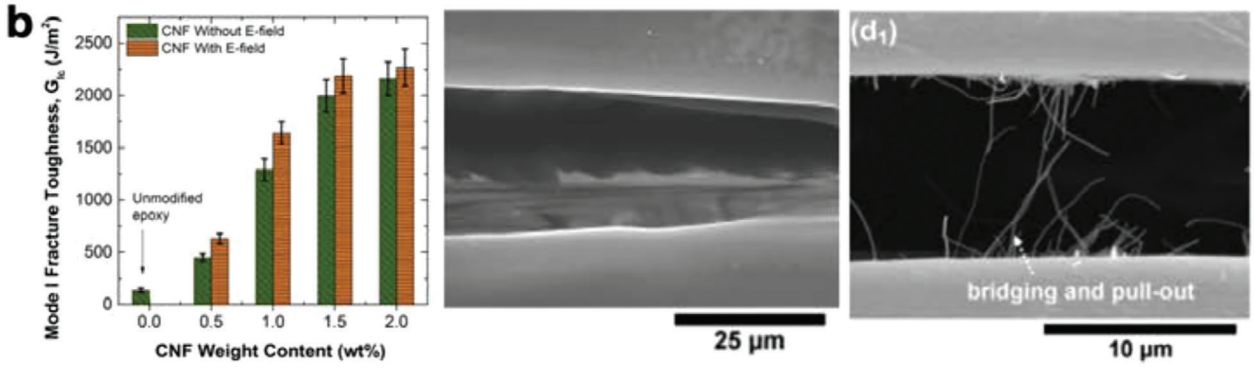

Grafting CNTs on carbon fibers

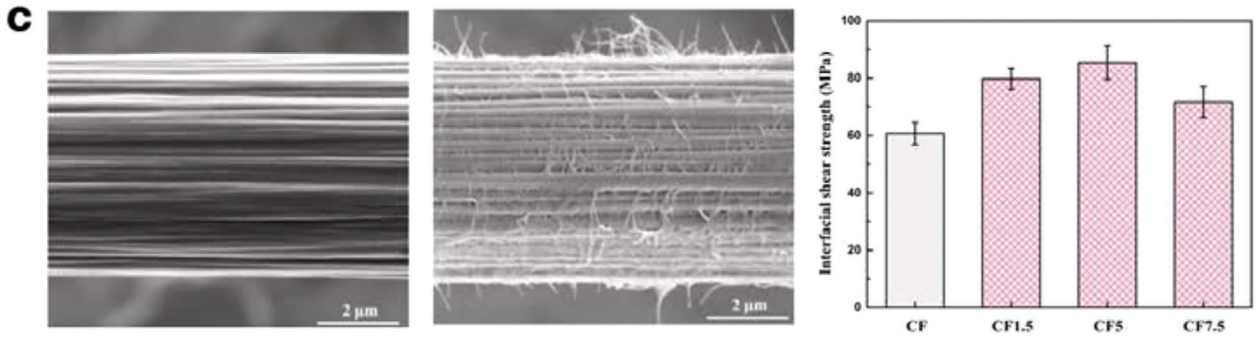

Macroscopic assemblies of nanoparticles (i.e. CNT forests)

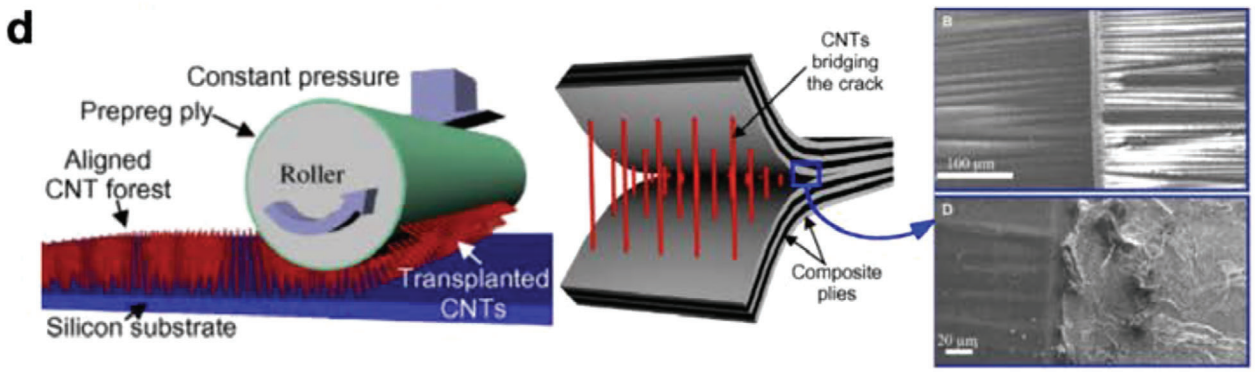

phase. While CNTs can improve interlaminar fracture toughness and reduce delamination crack propagation rates, their impact is often more pronounced during crack initiation rather than propagation. Achieving the desired toughening effect requires careful optimization of CNT concentration to avoid issues such as particle agglomeration. Additionally, achieving uniform dispersion of CNTs within the composite matrix is essential for effective crack bridging and toughening, but it can be challenging to attain.[7] Moreover, composites fabricated by this process generally suffer from low nanomaterial loadings (e.g., volume fractions typically <1%) because of manufacturing difficulties resulting from significantly increased resin viscosity associated with high nanofiller contents. Existing methods to increase nanofiller loadings include high-speed mixing, surface functionalization, and sonication, but these approaches can often damage the nanomaterials, counteracting their effectiveness.[127]

An alternative integration strategy involves grafting CNTs onto carbon fibers, potentially resulting in CNT bridging within CFRP laminates. As depicted in Figure 6c, grafted CNTs can protrude from the carbon fiber surface, establishing connections around neighboring fibers or between two laminae within the composite. Furthermore, CNT grafting significantly increases matrix/fiber shear strength due to the formation of robust chemical bonds and mechanical interlocking.[137,138] These connections between fiber layers can span across the cracks and delaminations, offering an extrinsic toughening mechanism through CNT bridging. For example, Sharma et al.[135] investigated the effect of grafted multi-walled carbon nanotubes (MWCNTs) on the flexural and interlaminar shear strength (ILSS) of carbon fiber-reinforced composites. The results indicated significant improvements compared to reference composites, with a remarkable 32% increase in flexure strength, while the ILSS increased by 35%. Fractographic analysis revealed that the primary fracture mechanisms in these composites included individual CNT pullout, CNT bundle pullout, and crack bridging by CNTs, alongside conventional interface debonding and fiber pullout. While grafted CNTs can provide additional strength and toughness through bridging, ensuring a consistent and controlled grafting process can be challenging. Additionally, the size and orientation of the grafted CNTs relative to the surrounding carbon fibers may affect their ability to effectively bridge cracks and contribute to toughening. Improperly grafted CNTs may lead to inconsistent mechanical properties across the composite, reducing the overall benefits of the grafting process.[137,139]

Developing more effective methods for integrating CNTs into composite laminates can significantly improve their performance. For instance, Wardle and colleagues[12] demonstrated that the use of vertically aligned nanotube forests can enhance delamination resistance in CFRPs. As shown in the schematic of Figure 6d, aligned CNTs were introduced between plies of a prepreg-based unidirectional tape laminate, creating a nano-engineered hierarchical architecture known as nanostitch. This method offers through-thickness reinforcement without the in-plane property changes typically associated with z-pinning and stitching. The vertically aligned CNTs facilitate resin infiltration, allowing for higher CNT loadings. The CNT forest ultimately functions as a reinforcing layer between the carbon fibers and the matrix, enhancing mechanical interlock and increasing the energy required to initiate and propagate a delamination crack. In particular, the authors observed a bridging effect, where the CNT forest provides a network of interconnected nanotubes that bridge the crack, slowing down or arresting crack growth. Besides, the presence of CNT bridges helps dissipate energy during crack propagation, thereby increasing the composite's delamination resistance. Blanco et al.[136] developed an analytical model to assess toughness improvement due to vertically aligned nanotubes. The model results indicated that the effectiveness is highly sensitive to the CNT aspect ratio, interfacial bonding with the matrix, and CNT volume fraction. Longer particles enable better crack bridging, while smaller diameters in the bridging zone model result in high stresses exceeding the strength of CNTs, thereby limiting toughness improvements.

3.2. Extrinsic Dissipation in Long Fiber Reinforced Composites

In the delamination process of composites reinforced with chopped fibers or CNT forests, extrinsic dissipation is usually exhibited on a small scale in the delamination tip. In advanced industries, like aerospace, long fiber reinforced composites are more widely used due to their demands for higher mechanical performance than civil engineering. In delamination of long fiber reinforced composites, extrinsic dissipation is exhibited on a large scale, even close to the structure size.[133]

The extrinsic dissipation in delaminating structures results in a rising resistance curve (R-curve). Delamination initiation is characterized by low fracture toughness associated with matrix or interfacial fracture. As delamination propagates further, long fibers are pulled out, creating a stable fiber bridging zone. Consequently, the total fracture toughness increases with crack size, and when a stable bridging zone develops, the total toughness reaches saturation. This saturation can be seen as the sum of the intrinsic interfacial toughness and the extrinsic dissipation due to large-scale fiber bridging (LSB).[52]

The origin and development of LSB have attracted interest from both academic and industrial fields due to its significant role in toughening the interface of laminated composite structures.[140] Many studies have shown that the origin of LSB can be attributed to the variability of interlaminar properties, including the randomness of microstructure and defects generated during the curing process.

Figure 6. Integrating carbon nanoparticles into composites enables the creation of multi-scale structures that enhance interlaminar fracture toughness. a) He et al.[130] used multi-layer resin infusion (MLRF) to stack resin films (embedding dispersed CNTs) with CF fabrics sequentially. An infusion process aligns CNTs, with DCB tests showing effective CNT pull-out and bridging. Reproduced with permission.[130] Copyright 2023, Elsevier B.V. b) Mixing carbon nanofibers into the epoxy matrix of carbon fiber-reinforced laminates enhances mode I fracture toughness. Reproduced with permission.[129] Copyright 2018, Elsevier B.V. c) Due to challenges in mixing CNTs with epoxy, alternative methods involve grafting CNTs onto carbon fibers. For instance, Wu et al.[138] reported a 40% increase in matrix/fiber shear strength due to improved hydrogen bonding and pinning effect at interphase region. Reproduced with permission.[138] Copyright 2022, Elsevier B.V. d) Wardle and co-workers[10] showed the bridging effect of adding a forest of aligned CNTs at the interlaminar interfaces of composite laminates. Reproduced with permission.[10] Copyright 2008, Elsevier B.V.

Frossard et al.[51] analyzed the effect of ply thickness on mode I interlaminar fracture behavior. Their study indicated that laminates made with thin plies (e.g., 0.03 mm) had a more uniform microstructure than those made of thick plies. As a result, a reduced amount of fiber bridging and lower fracture energy were reported, ranging from ~0.5 to 0.2 N mm^{-1}.

Curing conditions can also influence the heterogeneity over the interface due to low through-thickness thermal conductivity. For example, Hu et al.[141] studied the effect of curing thickness on the development of fiber bridging under mode I fracture. Samples made from thin curing plates (1 mm) exhibited less fiber bridging than those from thick curing plates (4 mm), with the average fracture energy dropping from 0.68 to 0.35 N mm^{-1}. Similarly, Chris et al.[142] demonstrated that the addition of a dwell stage before reaching the final cure temperature in thermoplastic particle interleaf toughened composites led to a reduction of up to 22% in Mode I toughness.

The development of LSB in laminated composites depends on their geometry, stacking sequence, and boundary conditions. Farmand et al.[50] discovered that thicker composite panels generate larger fiber bridging zones, resulting in higher propagation toughness, which increases approximately linearly with the DCB arm thickness. The reduced curvature in thicker specimens affects the decay rate of bridging traction and enhances fiber bridging. Additionally, recent studies have shown that the width of the delamination front significantly influences LSB development.[101] For 30°//30° interfaces, a delamination width of 20 mm led to more fiber bridging compared to 5 mm, as shown in **Figure 7**. The stacking sequence also plays a crucial role in extrinsic dissipation.[143,144] In multidirectional delamination, cracks can migrate into adjacent layers due to weak matrix properties.[145,146] For instance, Moura et al.[145] found that transverse cracking in 90° plies results in a zigzag delamination profile and an increased R-curve. Hu et al.[144] demonstrated a quantitative relationship between transverse cracking density and interlaminar toughness. Rehan et al.[146] observed that ply orientation impacts stable toughness but not initiation toughness, with significant variations in toughness for 45°//45° and 90°//90° samples due to fiber bridging. Moreover, Hu et al.[101,147] identified a linear relationship between mismatch angle and apparent toughness. Extrinsic dissipation, including fiber bridging and zigzag crack profiles, was evident under mixed-mode fracture.[148] Herráez[53] noted increased extrinsic dissipation with ply angle in pure mode II due to zigzag delamination, while Pichler et al.[54] reported that mode mixity also affects extrinsic dissipation in 45°// − 45° laminates.

Recently, the role of bridging has been highlighted in state-of-the-art 3D woven composites. These materials offer superior reinforcement in the thickness direction, leading to higher fracture toughness compared to 2D woven and traditional laminated composites. Xu et al.[149] evaluated the fracture toughness of these composites and reported a significant toughening effect, primarily due to the straightening and bridging of the fiber tow, alongside matrix shear failure and debonding between the fiber tow and matrix. This fiber bridging greatly enhances the damage resistance and fracture toughness. Given that 3D woven composites are currently being used for manufacturing fan blades and engine casings, the authors highlighted the beneficial role of bridging in hampering fracture propagation, which is critical for aero-engine blade containment.

The ability to control fiber bridging and harness it as a significant source of extrinsic dissipation is driving a paradigm shift in material design. Once considered merely an artifact of panel configuration and testing methods, fiber bridging is now recognized as a valuable opportunity to be directly leveraged in the design process. This aspect is particularly crucial in engineered composite materials, where the additional extrinsic toughening provided by fiber bridging becomes fully effective during impact loading and subsequent delamination. The enhanced toughness resulting from this process can be the critical factor that determines whether a material experiences catastrophic brittle failure or manageable ductile failure. Recent works support this view. Pascoe et al.[150] introduced a novel toughening concept using thin-ply reinforcements integrated into laminates as interlaminar reinforcements. These reinforcements consist of two plies of thin-ply prepreg with fibers oriented at 45 degrees to each other. Rectangular tabs are cut into one ply, and slits into the other, both aligned parallel to the fibers. When assembled, the tabs fit into the slits, creating a mechanically interlocked reinforcement unit. During delamination testing, these reinforcements are activated by the opening of the test specimens, effectively bridging the crack faces. Unlike typical fiber bridging, which involves numerous separate fibers connecting the crack flanks, this method confines bridging to well-defined bundles formed by the tabs, which remain intact and connect both sides of the crack. Out et al.[151] proposed using randomly distributed agglomerated CNT (carbon nanotube) particles as materials to toughen the interlaminar regions. These particles facilitate "extrinsic" toughening by enhancing fiber bridging. The authors noted that the randomly distributed particles functioned as discontinuous toughening phases, causing crack deflections. This significantly increases the crack propagation path and enhances fiber bridging, thereby improving the overall fracture performance.

In summary, controlling and harnessing fiber bridging as a significant source of extrinsic dissipation is transforming material design in composite structures. This paradigm shift is particularly crucial in advanced industries like aerospace, where enhanced toughness can prevent catastrophic failures. Recent innovations, such as the integration of thin-ply reinforcements[150] and the use of agglomerated carbon nanotube particles,[151] demonstrate the potential of fiber bridging to improve fracture performance. These advancements pinpoint the importance of fiber bridging in enhancing the toughness and durability of composite materials, paving the way for the development of more resilient and high-performance structures.

4. Strategies to Enhance by Design Extrinsic Dissipation in Adhesive Joints

In the previous section, we provided examples of fracture propagation where extrinsic dissipation plays a major role. This role is central, to the point that experimental observations could not be reproduced without introducing such a phenomenology. Long-span fiber bridging is one of the most telling examples for us, as its effect on toughening efficiency is remarkable.

It is therefore legitimate to wonder how one can draw inspiration from these observations to derive design principles that

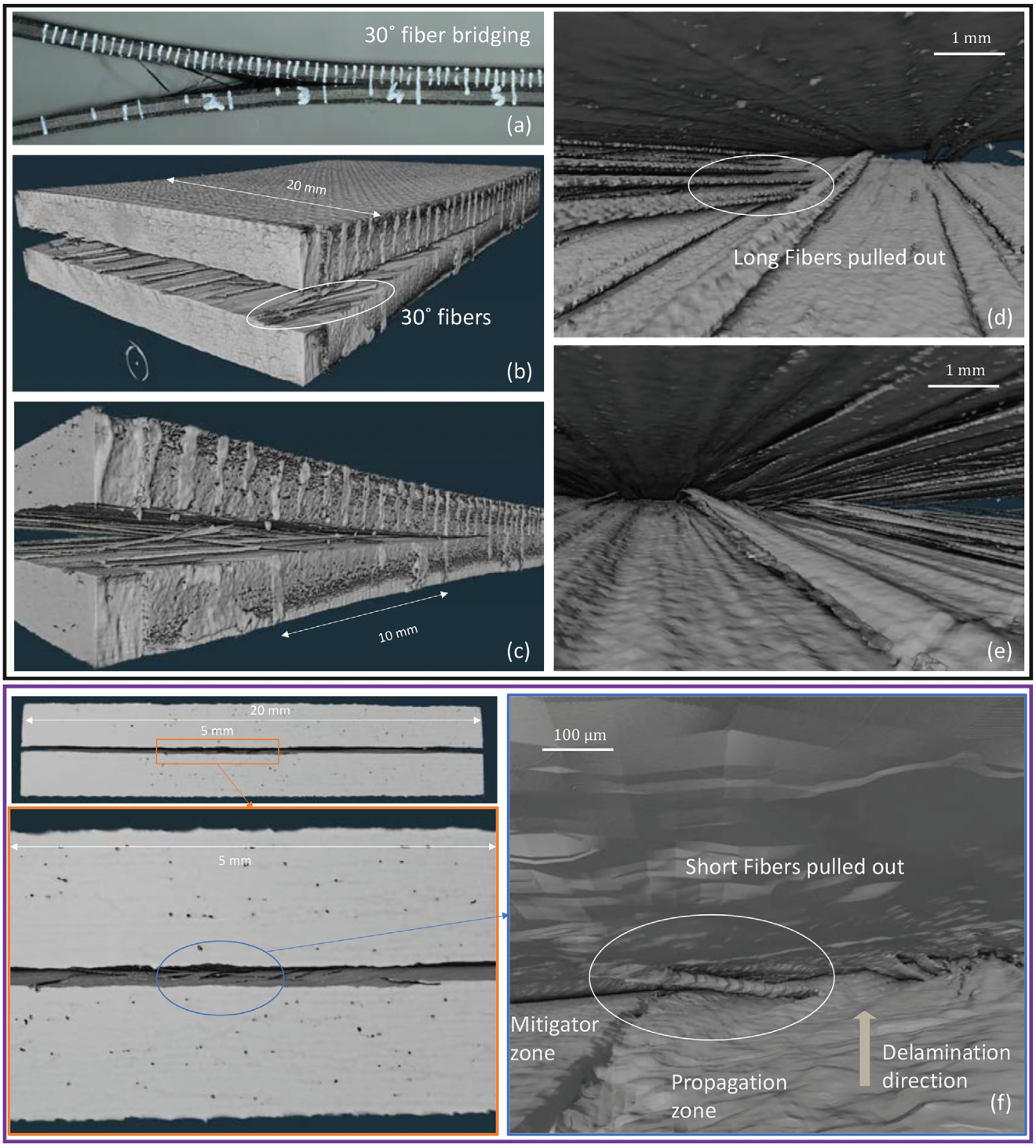

Figure 7. Delamination of multidirectional FRP (30//30) showing: a–e) Fully developed LSB in delamination width of 20 mm, and f) Short fiber bridging in delamination width of 5 mm. Reproduced with permission.[101] Copyright 2022, Elsevier B.V.

promote and control the extent of extrinsic dissipation. This is the focus of this section, illustrating successful approaches developed by the present authors and others in the context of composites and adhesive joints.

Adhesive joints in composites are made up of three components: (1) the parts to be assembled, which we will call the substrate, (2) the adhesive layer added to connect the parts together, referred to as the adhesive bondline, and (3) the

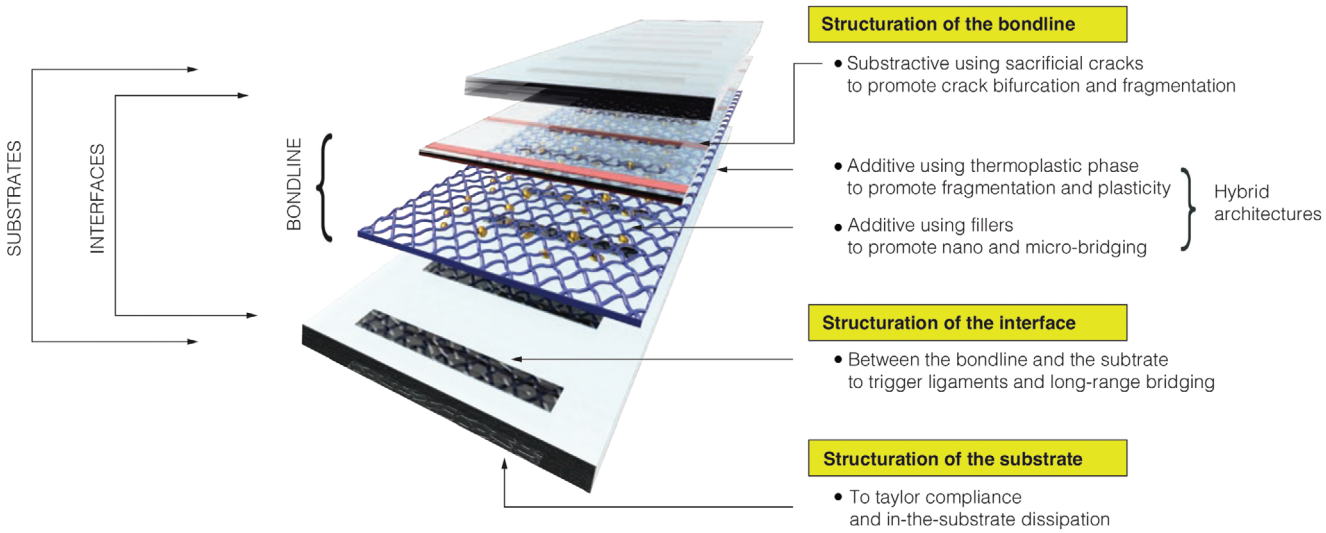

Figure 8. The various strategies used to enhance extrinsic dissipation in adhesive joints by structuring the bondline, the substrate or the interface in between the bondline and the substrate.

interfaces where the adhesive bondline connects to the parts. The discussed methodologies are grouped according to the assembly component targeted to trigger extrinsic dissipation, i.e., the interface, the adhesive bondline, or the mating substrates (**Figure 8**). While most techniques discussed herein are demonstrated on secondary bonded joints, it should be apparent that these methods can be generalized to laminated composite materials, where each interlaminar interface can be viewed as a joint.

4.1. Techniques Structuring the Interface Between the Bondline and the Substrate

Tao et al.[14] proposed a novel surface patterning strategy that promote extrinsic dissipation in the form of bridging adhesive ligaments. The idea stemmed from high-resolution in situ observations of fracture mechanisms in adhesively bonded composite joints whose mating surfaces were subjected to pulsed CO_2 laser irradiation.[152] A detailed experimental investigation revealed that local interfacial heterogeneities, such as loose fibers, led to a non-homogeneous adhesion landscape, which promoted the formation of adhesive ligaments capable of bridging the crack faces.[152] Additional analyses based on DCB testing demonstrated that ligament bridging can result in significant extrinsic dissipation (i.e., stretching and fracture of the ligaments), which greatly enhanced the ERR.[14]

Subsequent computational studies using the CZM within a finite element framework revealed that adhesive ligament formation can be more effectively controlled by tailoring the adhesion landscape of the composite adherents.[23] Specifically, a finite element model of a DCB specimen was developed, consisting of an adhesive layer (continuum elements) coupled by cohesive elements attached to the top and bottom adherents. These cohesive elements represented the adhesion at the CFRP/adhesive interfaces, with their properties adjusted to create a mismatch between the top and bottom interfaces. This mismatch was achieved by introducing patches with stronger adhesion (arrest regions) relative to the baseline across the interfaces, as illustrated in **Figure 9a**. A parametric study explored the effects of the position and degree of mismatch in these arrest regions. The simulations revealed three distinct failure modes: (a) no ligament formation during crack propagation (*NL*); (b) ligament formation without rupture during crack growth (*UL*); and (c) ligament formation followed by rupture during crack growth (*BL*). These modes are schematically depicted in Figure 9b and are fully dependent on the interfacial properties of the cohesive elements in the baseline and arrest regions.

In *NL*, the difference between the baseline and arrest interfaces is too small to stop crack propagation. In *UL*, the arrest interface causes the crack to jump from the bottom to the top interface, but the arrest interface lacks sufficient toughness, leading to simultaneous crack growth at both interfaces and large-scale ligament bridging. As the arrest interface properties increase further, the ligament fails in *BL*, where the crack transitions to the top interface after the initial jump. A detailed parametric study revealed that cohesive strength primarily influences *NL* and *UL*, while cohesive toughness is more critical for *BL*.[23] Additionally, geometric parameters such as the arrest interface size b and spacing distance g affect the overall energy dissipation.[23]

The proposed surface strategy was validated through experimental testing of composite DCB samples.[153] The experiments included both single and multiple arrest regions patterned across CFRP surfaces, as shown in **Figure 10a**. Such patterns can be created using various treatments like peel-ply removal, sanding, UV/ozone, plasma, and laser irradiation, provided a certain property contrast is maintained, as predicted by numerical analysis.[23] In our validation, both baseline and arrest interfaces were treated with pulsed CO_2 laser irradiation for its speed, precision, and ease of control. DCB tests demonstrated effective crack arrest and enhanced ERR, as shown in Figure 10b,c.

For illustration, the case *MP*2, which involves multiple patterning with a gap of $g = 2.5$ mm, was selected to demonstrate the mechanics of crack propagation. The results are shown in Figure 10d,e. After initiation at point 1, a large-scale bridging

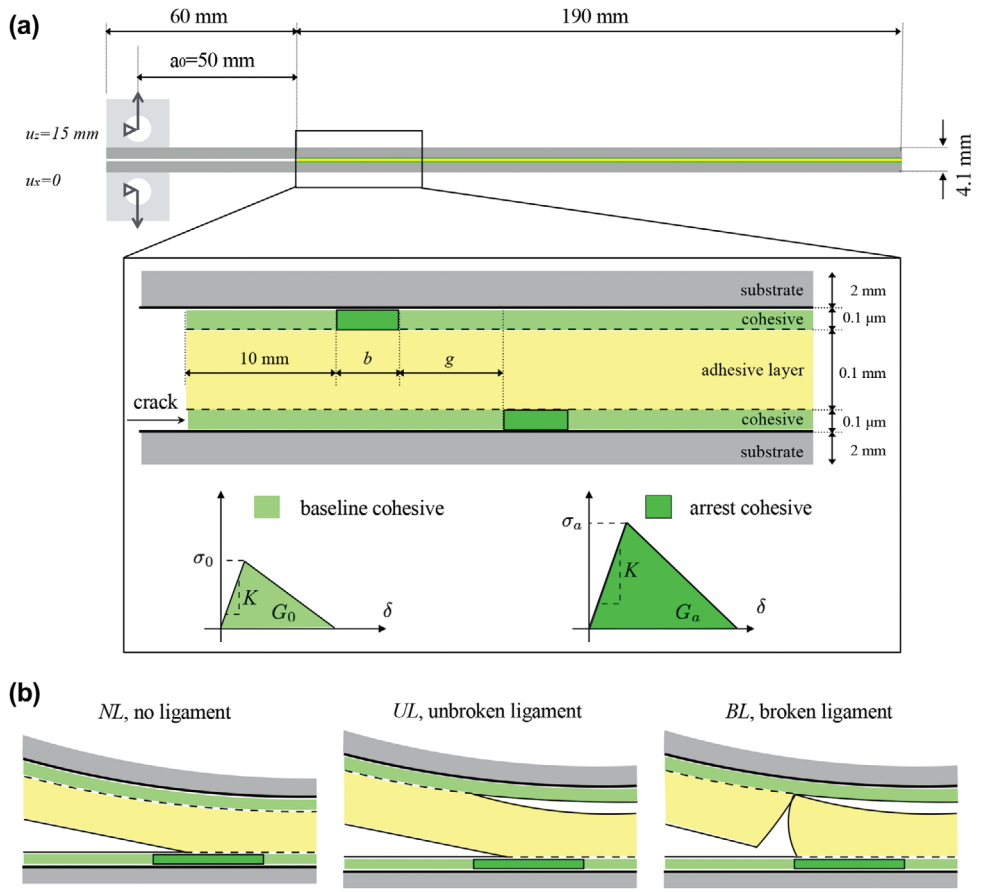

Figure 9. Techniques structuring the interface between the bondline and the substrate. a) Schematic of the 2D numerical model of surface alternative patterning strategy. The displacement control is applied to the bonding blocks. Parametric study included the patterning size *b*, gap distance *g*, baseline cohesive properties σ_0, G_0, and arrest cohesive properties σ_a, G_a. b) Schematic of three distinct failure modes depending on the interfacial properties: *NL*, *UL*, and *BL*. Reproduced with permission.[23] Copyright 2020, Elsevier B.V.

phenomenon occurs, resulting in an expanding bridging zone where up to three ligaments can simultaneously hold. Beyond point 3, the ERR curve reaches a plateau with fluctuations depending on the number of active bridging ligaments. Additionally, the bridging ligament may peel off backward to a previous arrest region on the opposite interface, as highlighted by the red circle in Figure 10e. At point 6, a larger enhancement is observed, with four ligaments holding simultaneously. Finally, ligament breakage occurs at point 7, leading to catastrophic failure. On the energy decomposition curve, the total structural energy U_t significantly increases, deviating from the dissipation of the CFRP/adhesive interfaces (U_d) from point 1, ending up 162.9% higher. Finite element results indicate that most of the enhanced total energy is stored elastically in the bridging adhesive ligaments. Triggered adhesive ligaments significantly enhance ERR in mode I DCB joints, with more bridging ligaments resulting in a higher plateau value. Two mechanisms contribute to this enhancement: first, bridging ligaments formed at multiple damaged interfaces slightly increase ERR values as the crack propagates; second, a greater amount of strain energy is needed to bend and stretch these ligaments further.

The proposed patterning strategy is designed to structure the interface as a crack arrest feature, effectively stopping crack propagation and improving ERR. Both numerical analysis and experimental investigations confirmed the controlled triggering of adhesive ligaments. However, the brittleness of the thermoset epoxy adhesive exacerbated unstable crack propagation after ligament failure, which pinpoints the need for additional research to refine the methodology.

4.2. Techniques Structuring the Bondline

The toughness of an adhesive system can also be enhanced by modifying the structure of the adhesive layer so more dissipation will take place within the bondline. Maloney et al.[154] proposed a stopping hole structure, deliberately creating an array of holes in the bondline to periodically arrest crack propagation. This stopping mechanism was inspired by the work of Makabe et al. and Murdani et al.[155,156] who demonstrated that such stop holes can blunt the stress singularity at the tip of a sharp crack, thereby enhancing the fatigue strength of aluminum parts. In adhesive joints, when the crack reaches the stopping holes, a reduction in load and toughness occurs. However, energy and force recover once the crack length surpasses the hole diameter, as a new crack initiates after the hole, dissipating significant energy.

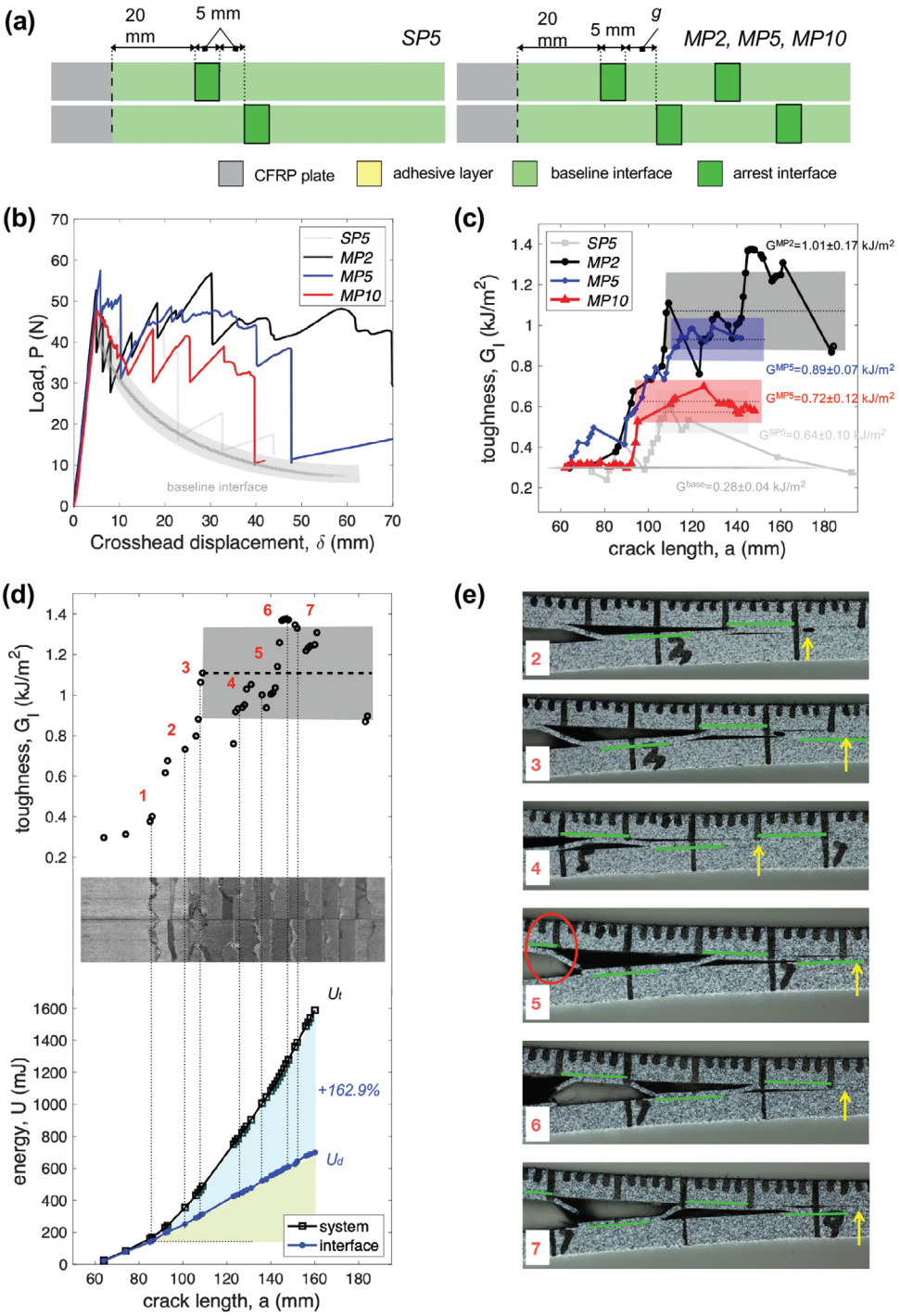

Figure 10. Techniques structuring the interface between the bondline and the substrate. a) Schematic of both single and multiple surface alternative patterning strategy. *SP*5 is single patterning with *g*=5 mm, *MP*2 is multiple patterning with *g*=2.5 mm, *MP*5 is multiple patterning with *g*=5 mm, and *MP*10 is multiple patterning with *g*=10 mm. b) Load-displacement curves of *SP*5, *MP*2, *MP*5, and *MP*10. c) ERR curves of *SP*5, *MP*2, *MP*5, and *MP*10. The baseline curves indicated the values obtained from uniform baseline interfaces. d) ERR curve, corresponding energy decomposition, and e) in situ crack propagation observations of one typical *MP*2. Reproduced with permission. Copyright 2020, Elsevier B.V.

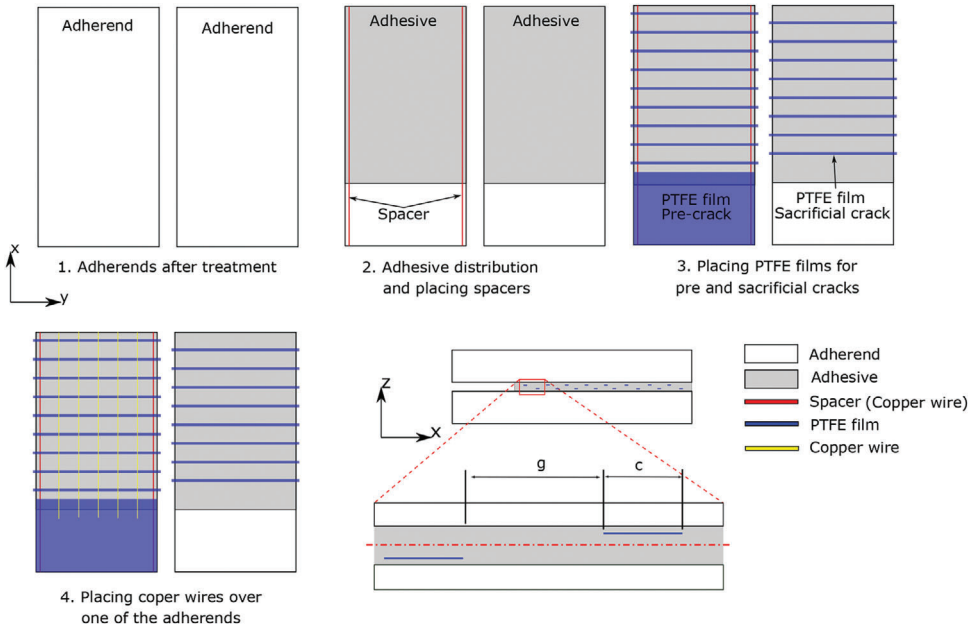

Figure 11. Subtractive techniques structuring the bondline. Schematic of the manufacturing process of bio-inspired adhesive modified with sacrificial cracks. Reproduced with permission.[157] Copyright 2021, Elsevier B.V.

Consequently, the macroscopic fracture energy of the system increases. By varying the hole diameter, spacing between holes, and adhesive thickness, Maloney et al. demonstrated up to a 50% enhancement in toughness. They also proposed a second method for structuring the adhesive layer using a copper wire mesh. The presence of the mesh in the bondline allows the formation of adhesive ligaments that dissipate large amounts of energy during deformation, leading to a further enhancement in toughness.

Other methods described in recent literature, along with detailed discussions of the dissipation mechanisms during crack propagation that contribute to toughness improvement, are discussed further below. Approaches based on bondline structuration techniques provide a fundamental advantage: the bondline can be engineered as a separate product and used for the assembly of the parts, without modifying these directly. Such techniques are therefore non-invasive and can be integrated into the fabrication process with relative ease.

4.2.1. Subtractive Techniques: Sacrificial Cracks

A novel technique, bio-inspired adhesive, was inspired by one of the sea living that has an excellent adhesion toughness, *Mytilus californianus*, by embedding sacrificial cracks within the adhesive layer.[157] The sacrificial cracks were embedded inside the adhesive bondline with offsets from the central axis using a Polytetrafluoroethylene (PTFE) film, which has a low adhesion with adhesive as shown in **Figure 11** to simulate the presence of voids in the microstructure of the *Mytilus californianus* bondline. To manufacture such a joint, the adhesive should be applied to both adherend surfaces. PTFE strips with a width, *c* are applied to both adhesive layers with a gap between two successive sacrificial cracks, *g*. The toughness improvement was demonstrated under mode I[157] and II[158] fracture toughness using standard DCB and ENF tests. An effective crack length method, based on the Timoshenko beam theory, was used to compute the fracture toughness under mode I[159–161] and II[162,163] due to the difficulties in determining the crack tip (several crack tips grow at the same time). Under mode I, the sacrificial cracks lead to the crack bifurcation between both sides of the bondline, in contrast to traditional joints that suffer interfacial failure, which happens at one of the substrate/adherend interfaces. Consequently, secondary and backward cracks spread at the lower and upper interfaces beneath and over the sacrificial cracks, respectively. When the main crack (propagating at the lower interface in **Figure 12**) reaches the first sacrificial crack, a new crack initiates at the upper interface forming an adhesive ligament between the upper and lower interface. By increasing the deformation, not only the main crack grows but also the secondary crack that has initiated grows, which increases the toughness of the system. This adhesive ligament stores elastic energy and dissipates energy due to plastic deformation during loading. The elastic energy is released once the ligament is broken, which causes a load and toughness drop (see Figure 12), while the plastic dissipated energy contributes to the toughness improvement. Under shear mode, the toughening mechanisms are almost the same, where crack migration between the upper and lower interface of the bondline was observed, which forms adhesive ligaments that lead to secondary and backward crack propagation. However, the adhesive ligaments in this testing case do not break, they keep deforming until complete propagation of the crack.

The toughness of the joint modified with sacrificial cracks is dependent on several parameters such as the bondline thickness, the sacrificial crack topology (the length and the gap between successive cracks), and the properties of the adhesive. The adhesive bondline thickness affects the initiation and propagation of the crack and thus affects the fracture toughness of the joint. Generally, for all the considered adhesive thicknesses in the literature

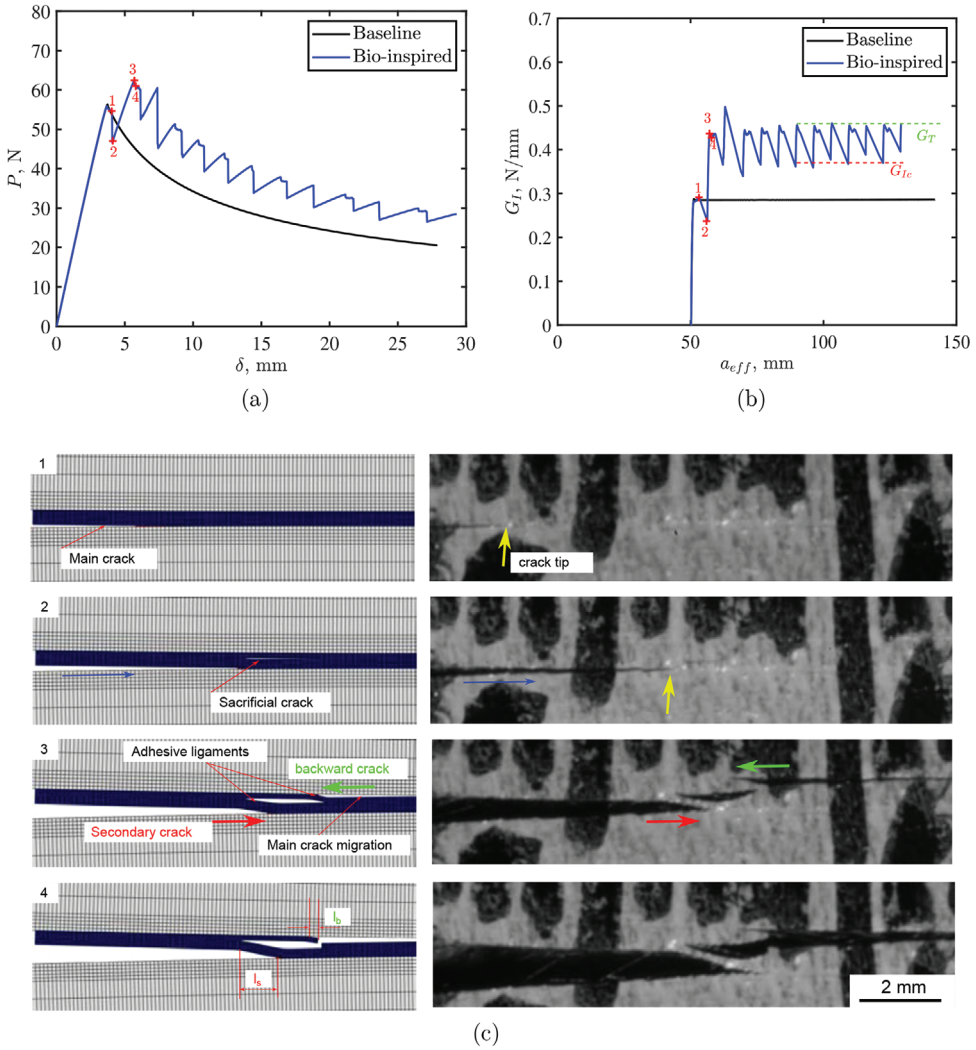

Figure 12. Subtractive techniques structuring the bondline. Damage evolution in bio-inspired adhesive joint: a) $P-\delta$ curve, b) R-curve and c) damage modes at different loads marked in a. Reproduced with permission.[157] Copyright 2021, Elsevier B.V.

that vary from 0.25 to 1 mm, the fracture toughness of the joint with sacrificial cracks is larger than the baseline joint. However, the thinner the thickness is the higher the toughness improvement is.[158] This is due to the small thickness of the adhesive which allows for strain localization at the crack tip higher than the thick adhesive in the baseline joint. When sacrificial cracks are embedded in the adhesive system, the energy required to redistribute the stresses between the three crack tips (the main tip and the two tips of the sacrificial cracks) is larger in the case of thin than thick adhesives. This conclusion might be dependent on the given properties of the constitutive material and need to be validated with a careful parametric study for each material. The sacrificial crack length and the gap between two successive cracks significantly affect the toughness of the joints, where the smaller the crack length is, the larger the toughness is. This makes sense because the small crack length allows longer propagation of the secondary and backward cracks during propagation, which dissipates larger energy. The toughness of the joint is less sensitive to the gap between two successive cracks than the crack length, where the gap contributes more to the number of ligaments generated in a specific length of the joint, and thus the amount of energy dissipated as plastic deformation in the joint. The adhesive properties also play an important role in the toughness of the joints modified with sacrificial cracks. Increasing the adhesive strength and/or the failure strain increases the toughness of the adhesive joint modified with sacrificial crack due to the delay of the failure of the adhesive ligaments, which allows for longer propagation of the secondary and backward cracks. However, for the baseline joints, the bulk adhesive properties do not play a vital role in the toughness of the joint because the toughness of the joint is mainly governed by the interfacial interaction at the interface between adhesive and adherend.

4.2.2. Additive Techniques: Hybrid Architecture

The concept of hybrid architecture adds foreign insert/carrier into the adhesive bondline, creating hybrid bondline that holds

two adherends together.[24,25,154,164–167] Hybrid architecture activates an extrinsic dissipation through the introduction of new interfaces between dissimilar materials. This extrinsic dissipation culminates in an enhancement of fracture toughness, through bridging mechanisms by the ligaments/strands that reduce local stress and strain fields at the vicinity of crack tip.[168]

Aspects that ensure the effectiveness of the insert include architecture, geometry, topology, arrangement, and materials. We illustrate this approach by two efficient techniques: the first one is based on the integration of a pre-designed thermoplastic phase, while is the second one based on the enrichment of the bondline with nanoparticles that promote bridging and fragmentation.

By integration of a thermoplastic phase. Integrating a thermoplastic strip made of polyvinylidene fluoride (PVDF) of 1 mm width and 0.125 mm thickness into epoxy adhesive (Loctite AE96950.05 PSFK) bonded between two carbon/epoxy (IM7/8552) adherends was proposed in Ref. [164]. An experimental investigation using a DCB showed that the PVDF strip was able to increase mode I fracture energy G_{Ic} from 0.73 to 2.1 N mm^{-1}, leading up to the toughness enhancement of nearly 200%. Here, the PVDF strip acted as a crack inhibitor that strongly delayed the crack growth, promoting significant toughness enhancement. However, incorporating PVDF strips was ineffective in improving the shear strength of the bondline, which was studied by performing single-lap shear test. The shear strength of specimens with PVDF strip was 17% lower than that without PVDF strip due to the strip positioning issues that were encountered during the bonding process. Due to pressurization, the strip displacement inside the bondline squeezed out the epoxy, reducing the bonding area between two adherends. The limited bonding area activated an adhesive failure (failure between substrate and adhesive) that triggered a premature failure. Integrating a thermoplastic feature in the bondline was successful when the feature was still in a nearly-cured condition and directly laid on the composite layer. This was demonstrated using 3D printing technology to print thermoplastic features directly on the composite layer of a single-lap shear specimen.[165] The 3D-printed strips made of acrylonitrile butadiene styrene (ABS) with a width of 700–800μm were laid in the middle portion of the bondline perpendicular to the loading direction. As a result, the shear strength of the joint was improved by 800%. Although bridging ligaments were not evident, the primary mechanisms responsible for this were attributed to the shift from adhesive failure to the cohesive failure (failure within the adhesive).

The role of bridging ligaments as a primary extrinsic toughening mechanism was demonstrated by inserting a foreign insert with a more complex architecture into the adhesive bondline (epoxy) between composite adherends.[24,25,154,166] Some examples of additive techniques for triggering extrinsic dissipation are shown in **Figure 13a–c**. Figure 13a shows that incorporating a wavy nylon insert could improve G_{Ic} by 100–400% depending on the adhesive amount used.[24] Less adhesive produced a higher porosity due to the unfilled spaces within the insert (i.e., pores), which activates the multiple strands to bridge between substrates by promoting stretch-and-breaking mechanisms. The crack bridging by nylon strands is an evident extrinsic toughening that eventually produces higher toughness. Similar concept was also reported in Ref. [25] where an array of straight, multiple nylon wires (width = 1 mm) were able to improve G_{Ic} by 75–320%, raising the nominal G_{Ic} from (sample without insert) to 1.68 N mm^{-1} (sample with insert). The optimum spacing between wires (number of wires per sample) that maximized G_{Ic} was 3 mm as the wires varied crack path as a result of weak adhesion between nylon wire and epoxy adhesive, enabling the transition from brittle failure toward ductile failure of the nylon wires. A 2D mesh with a diamond-celled lattice knit pattern made of nylon (40–50μm diameter) came together within the epoxy film (AF163-2k) as a thickness-controlling feature and was used to bond two carbon/epoxy (AS4/8552 Hexply) substrates.[166] Figure 13b shows that the crack growing at the bondline was bridged by the nylon ligaments, introducing extrinsic toughening (referred to as bridging energy release rate G_b) with oscillating R-curve at the average of 1 N mm^{-1}. Bridging ligaments by the insert were observed for the adhesively bonded joints embedded with a metallic mesh/insert made of copper as shown in Figure 13c.[154] As the crack attempted to grow at the bondline, the copper mesh promoted two competing mechanisms: interfacial failure and crossing of the crack tip toward the opposite interface. In this process, the crack grows in a zigzag manner, generating multiple bridging ligaments that eventually give rise to the fracture toughness improvement of 160%. Adding a metal mesh was also proven effective in doubling the SLJ strength of carbon/epoxy.[167] The metal mesh in the bondline of SLJ specimen acted as an adhesion promoter that induced the interplay of three mechanisms: adherend failure, bridging and anchoring between metal meshes, and stress redistribution at the crack tip.

By integration of nanoparticles, example of CNT spraying. A simple approach to achieving high-performance interfaces is through the spraying of nanofillers, including CNTs. On the one hand, spraying happens to be a quite cost-effective process, requiring only low-cost facilities and easy to upscale. On the other hand, it often comes with safety concerns due to the volatility of the cloud of nano particles and to the usage of various solvents. For instance, solvent spraying of CNTs onto carbon fabrics has been employed, resulting in improved shear strength.[169] Another study introduced MWCNTs by spraying them onto Teflon-coated peel cloths and subsequently transferring them to woven prepreg plies, resulting in a 32% increase in mode-I fracture toughness.[170] Furthermore, Mujika et al.[171] reported a 14% increase in mode-II fracture toughness by spraying an ethanol solution of MWCNTs and conducting end-notch flexure testing on both neat and reinforced samples. Due to the significance of mode-I fracture toughness and its ability to drive most critical failure mechanisms, Almuhammadi et al.[172] conducted a specific study addressing mode-I nano-reinforcement. They sprayed MWCNTs onto UD prepreg plies and explored the microscopic mechanisms of failure that lead to modifications in interlaminar fracture toughness. Ensuring the well-dispersion of MWCNTs, as confirmed by Raman mapping and SEM of the fractured surface, is essential.

Several aspects must be addressed when employing the nanofiller spraying method to achieve high-performance interfaces. One key aspect of using nano-reinforcement, especially with the spraying method, is the uniform dispersion of nanofillers to maintain a good distribution of reinforcement on the targeted surface. Additionally, it is crucial to select a liquid medium with good wetting compatibility with the targeted

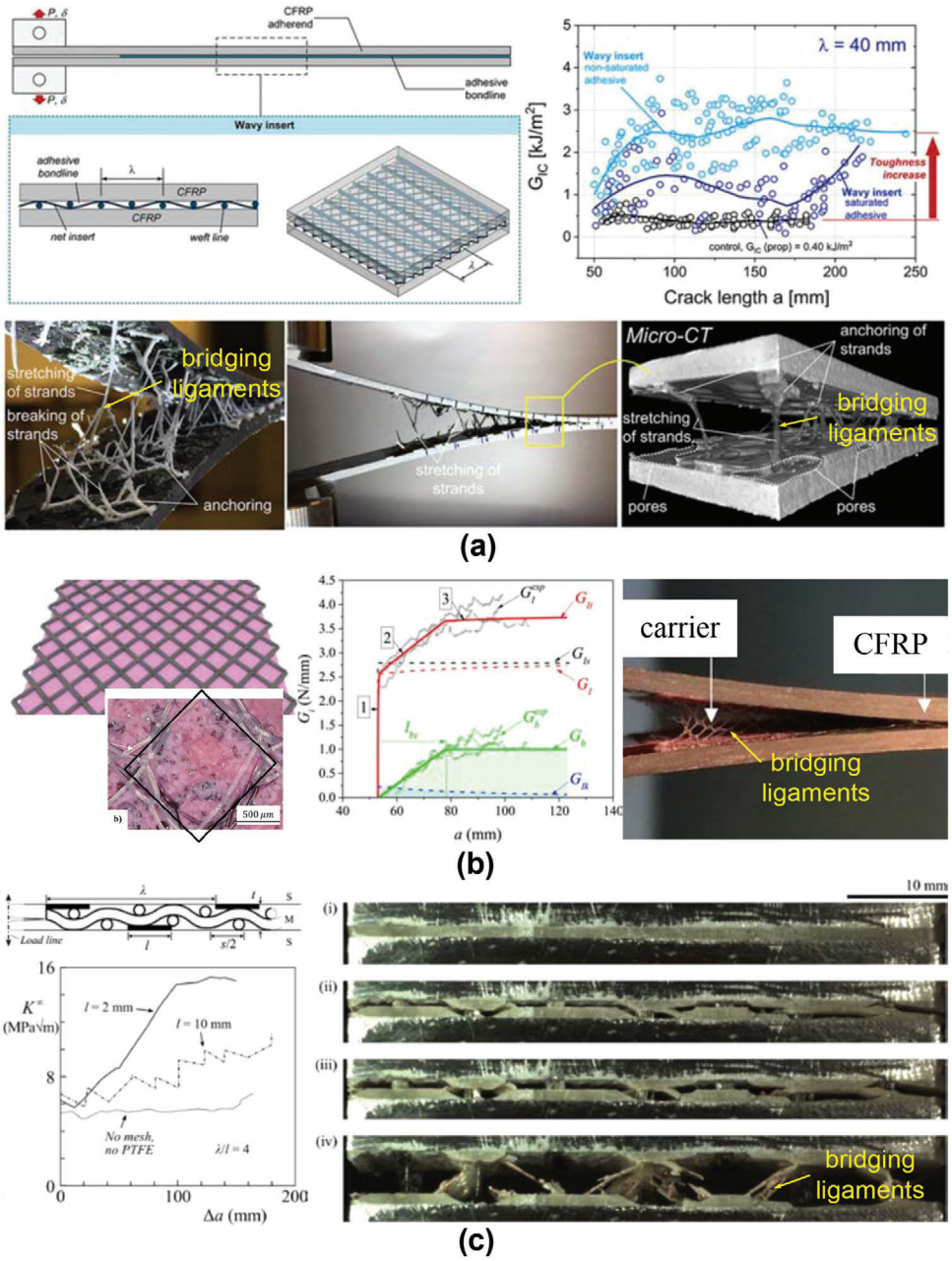

Figure 13. Additive techniques structuring the bondline. Triggering extrinsic dissipation via the activation of bridging ligaments: a) Nylon wavy insert. Reproduced with permission.[24] Copyright 2020, Elsevier B.V. b) Nylon carrier. Reproduced with permission.[166] Copyright 2018, Elsevier B.V. c) Copper mesh. Reproduced with permission.[154] Copyright 2019, Elsevier B.V.

ply surface, as well as ensure good chemical compatibility.[172] In summary, applying nanofillers such as CNTs and MWCNTs via spraying methods has significantly improved both mode-I and mode-II fracture toughness. The uniform dispersion of nanofillers and the selection of an appropriate liquid medium are critical factors for optimizing the reinforcement effects. These findings highlight the potential of nanotechnology in enhancing the mechanical properties of composite materials. As research in this area progresses, it is expected that the integration of nanofillers will play a crucial role in developing next-generation high-performance materials with superior interfacial properties.

4.3. Techniques Tailoring the Substrate

As illustrated in the previous subsection, the adhesive bonding community has been recently focusing on enhancing the damage tolerance of bondline materials in laminated structures[14,152] by modifying the adhesive composition, such as incorporating

a ductile second phase (e.g., a bridging phase), including a knit polyamide carrier,[28] copper mesh,[173] a 3D-printed wavy net-like polyamide insert,[24] polyamide fibers,[25] or by enabling the formation of adhesive ligaments.[23,153] These additions help absorb energy during fracture. However, with recent global initiatives promoting sustainable manufacturing and material use, improving performance solely through adjustments in material chemistry and composition has become a challenging pursuit. Consequently, there has been a shift toward extrinsic approaches centered around adherend architecture.[174]

As depicted in **Figure 14**, recent studies by the authors and others have demonstrated that adherends can be intentionally designed with specific internal structures, such as patterns, channels, or voids. This design approach aims to enhance bonding strength and increase fracture resistance, irrespective of chemical composition—additionally, in some instances, it facilitates lightweighting strategies.[174–180] This concept becomes clearer when considering the cohesive length scale (ℓ), which is influenced by key mechanical properties like Young's modulus (E), cohesive strength (σ_f), and fracture toughness quantified by the critical ERR ($\mathcal{G}_{Ic}$):

$$\ell \approx \frac{\mathcal{G}_{Ic} E}{\sigma_f^2} \rightarrow \mathcal{G}_{Ic} \approx \frac{\ell \sigma_f^2}{E} \tag{4}$$

The equation above demonstrates how fracture energy can be increased by either reducing Young's modulus (E) or increasing characteristic length (ℓ) and failure stress (σ_f). While these properties are interconnected and any modification involves changes in composition, the effective Young's modulus can be manipulated through careful control of the adherends' geometry. Therefore, tailoring the architecture of the bonded layers can result in increased toughness and improved damage tolerance in laminated structures.

Inspired by the work of Kendall,[181] Xia et al.[175,176] studied the peeling of thin, flexible films with varying thicknesses along their length. Their work, which is summarized in Figure 14a, revealed that differences in elastic stiffness can improve fracture toughness in heterogeneous materials. The peeling process slowed down as the peeling front neared the boundary between the more flexible and stiffer regions, causing a peak in the applied peeling force. Further loading led to a sudden crack propagation and a drop in load, indicating snap-through instability. In a later study, Hsueh et al.[182] found that this improvement was due to stress fluctuations that resulted in areas where the stress intensity at the crack was significantly lower than the overall applied stress. These unstable transitions produced serrated load versus displacement responses, similar to stick-slip behavior seen in the delamination of composite laminates and tribology.

More recently, Morano et al.[177] explored crack propagation in DCB adhesive joints with constant thickness adherends, featuring subsurface channels inspired by the shell of the barnacle *Amphibalanus amphitrite*. The channels modulated the bending stiffness and promoted a snap-through cracking process, mirroring the pinning/depinning process observed in patterned thin films. Morano et al.[180] further demonstrated that adjusting channel geometry can control crack propagation and energy dissipation, enabling crack shielding and delayed growth, as well as unlocking additional energy-absorbing processes such as interfacial void growth and buckling. Luo and Turner[178] investigated a similar model material system consisting of a DCB specimen with elastic heterogeneity beneath the substrate's surface. Their findings closely matched those of Morano et al.[177] They have shown that introducing structured stiff insets modified the mechanical properties and adhesion of compliant beams, affecting stress distribution and the response at the adhered interface. Stiff insets improved effective adhesion, especially when exceeding a critical length, i.e., spacing of the insets less than 1.5 times the height of the beams enabled increased adhesion.

It is worth noting that each non-equilibrium transition (i.e., snap-through) occurring as the crack advances releases energy that is not recovered but converted into elastic waves, transmitting kinetic energy throughout the specimen, where it dissipates as heat, vibrations, and acoustic emissions.[173,183] This mechanical dissipation increases the total energy involved in the fracture process. In this context, Alfano and co-workers[184] have investigated the snap-through crack propagation using a mechanoluminescent coating. They applied a mix of pre-synthesized green-emitting $SrAl_2O_4/Eu^{2+}$ particles and epoxy to selected DCB joint surfaces using an airbrush. This coating produced green light (at λ_{em} = 520nm) proportional to applied stress, visualizing dynamic stress distribution during crack propagation. Time-resolved emission patterns showed significant bursts of light intensity at each crack pinning/depinning transition, originating from the crack front region and extending to much of the DCB, both in the wake and ahead of the crack. The variation in light intensity was linked to sudden shifts in crack growth rate and appears to confirm earlier work that speculated the emission of speed waves.

This body of research shows how customizing the architecture of the mating layers enhances the mechanical performance of laminated structures. By precisely adjusting the geometrical properties of subsurface regions adjacent to the interface, laminates can be strengthened, allowing for enhanced energy dissipation without altering key joint attributes like the interface or bondline composition. The potential for advancement in this area is significant, particularly with the integration of additive manufacturing technologies. These advanced methods enable the fabrication of intricate mechanical components across a range of materials, from polymers and metals to composites. This convergence of techniques promises to drive innovation in the design of laminated structures, reshaping established practices and broadening the scope of engineering design.

5. Modeling of Extrinsic Responses in Laminated Structures

In Section 2, we provided a brief overview of classical modeling and identification techniques in cases where dissipation stems from intrinsic mechanisms. In such approaches, dissipation is solely determined by the local opening and kinematics of the crack tip, and the critical ERR (as known as the fracture energy) appears to be a material property. However, in many situations, this intrinsic approach is not applicable, as other mechanisms come into play that can dissipate a significantly larger amount of energy. As detailed in the previous section, extrinsic effects

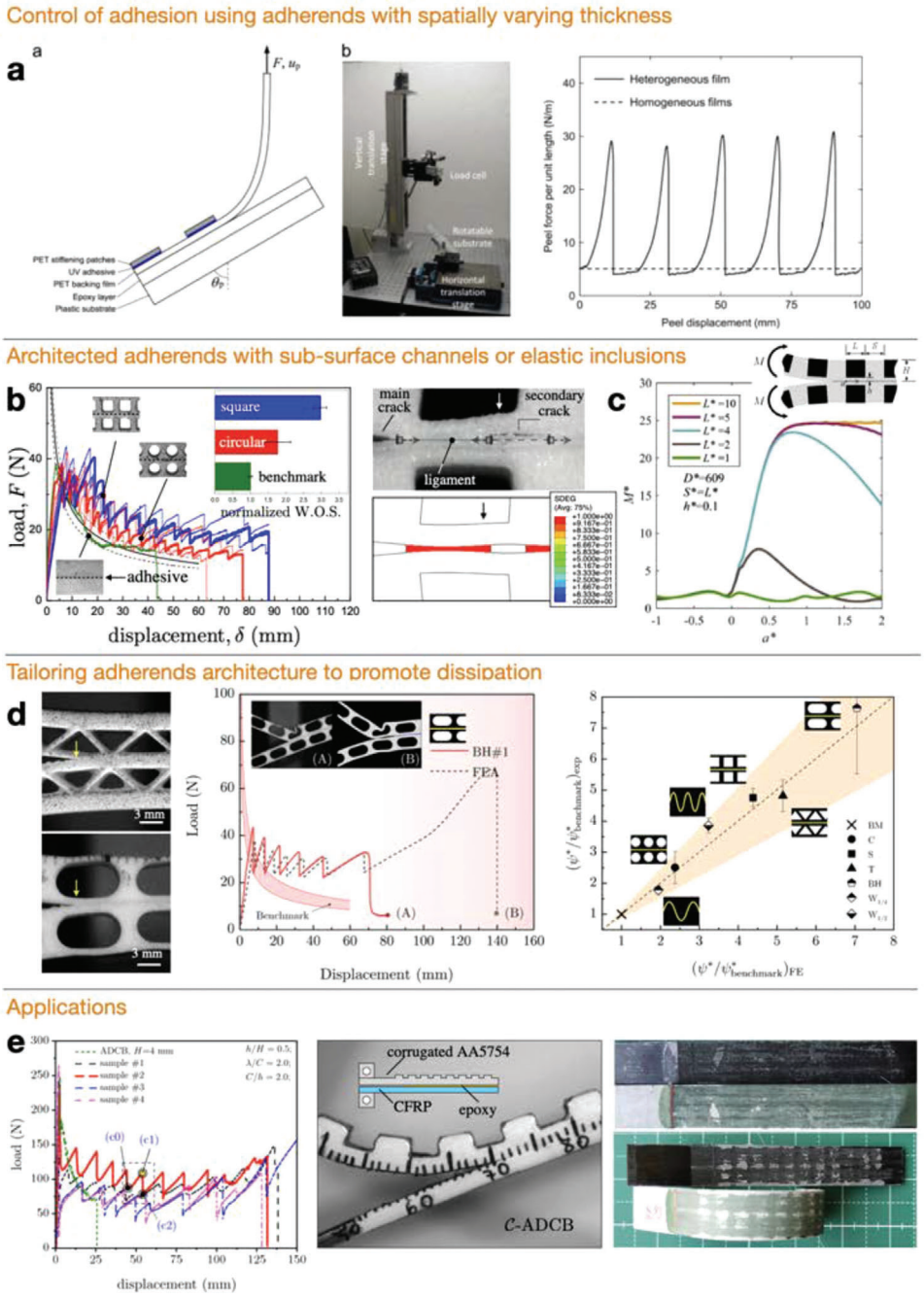

Figure 14. Substrate tailoring for improved dissipation. a) Xia et al.[175,176] studied how varying thicknesses of thin, flexible films induce a snap-through instability and enhance fracture toughness in heterogeneous materials. Reproduced with permission.[176] Copyright 2013, Elsevier B.V. b) Morano et al.[177] investigated crack propagation in DCB adhesive joints with subsurface channels inspired by the barnacle *Amphibalanus amphitrite* shell, promoting snap-through cracking by modulating bending stiffness. Reproduced with permission.[177] Copyright 2020, Elsevier B.V. c) Luo and Turner[178] confirmed these findings with a similar DCB specimen featuring elastic heterogeneity. Reproduced with permission.[178] Copyright 2022, Elsevier B.V. d) Adjusting the channels' geometry allows the harnessing of additional energy-absorbing processes like buckling and void growth. Reproduced with permission.[180] Copyright 2023, American Chemical Society. e) Morano et al.[185] utilized corrugated adherents to control crack propagation and enhance energy dissipation in adhesive bonded composite/metal joints (up to 260%) compared to non-corrugated adhesive joints). Reproduced with permission.[185] Copyright 2022, Elsevier B.V.

might result in large modifications of the fracture properties. Especially the toughness might vary a lot depending on the extent of non-local mechanisms such as bridging. Modeling such effects is far from trivial as it results in non-local modeling accounting for the kinematic of the structure in the response at the material point level. We present in this section recent efforts that have been made in this direction.

5.1. Bridging Effects

Significant efforts have been made toward a more accurate prediction for delamination with LSB and other extrinsic mechanisms happening in interphase, primarily through the utilization of CZM-based methodologies. One class of such efforts is to modify the TS laws of CZM to achieve a better match of the *R*-curve behaviors between the predictions and excremental results.[186–189] Tuning the TS laws gives satisfactory predictions when applied to benchmark tests whose loading condition is simple and the configuration of FPZ (width, length, etc.) is consistent throughout the delamination process. However, in more general cases, energy dissipation mechanisms during the delamination may not only depend on the local characteristic of the interlaminar properties but also on the status of FPZ[56,190] and other factors, such as the geometrical configuration,[27,101,191,192] the propagating direction,[37,193,194] the ply orientations,[55,195,196] the processing parameters,[100,197] etc. Hence, the delamination resistance of a laminate, referred to as the apparent fracture toughness, depends on various parameters associated with the spatio-temporal feature of the FPZ. This broader contribution forms the extrinsic dissipation and is difficult to quantify in modeling.

To probe how the geometry of FPZ affects energy dissipation, Pappas and Botsis[56] conducted experiments using DCB specimens under various loading conditions. They revealed that different deformation statuses of FPZ may result in different processes of fiber bridging, which is attributable to differences in crack opening curvature. This can modify the overall energy dissipation of delamination, leading to different apparent fracture toughness.

To enhance the modeling of this phenomenon, they developed a novel CZM that incorporates the influence of local curvature. This advancement allows for a more accurate representation of the deformation mechanisms within the FPZ.[190]

Blondeau et al.[55] experimentally demonstrated higher delamination resistance for angle-ply interfaces than their unidirectional counterparts, highlighting the effect of interface ply orientations and delamination growth direction. Moreover, Hu et al.[101] identified the scale effect of the extrinsic energy dissipation, namely, the fiber bridging, delamination migration, and other related mechanisms are dependent on the geometrical configuration of the delamination front.

Therefore, the apparent toughness of delamination, denoted by $\mathcal{G}_{Ic}^{\mathrm{App}}$ can be decomposed into the intrinsic contribution $\mathcal{G}_{Ic}^{\mathrm{Int}}$ and the extrinsic contribution $\mathcal{G}_{Ic}^{\mathrm{Ext}}$ as follows:[147,198]

$$\mathcal{G}_{Ic}^{\mathrm{App}} = \mathcal{G}_{Ic}^{\mathrm{Int}}(\alpha_1) + \mathcal{G}_{Ic}^{\mathrm{Ext}}(\alpha_1, \alpha_2, \alpha_3, \ldots) \quad (5)$$

where α_1, α_2 and α_3.... are the factors that influence the extrinsic toughness. It is noted that some of the influencing factors, such as fiber orientation mismatch, may take effects on both intrinsic and extrinsic dissipation. Identifying the nonlocal characteristics of extrinsic dissipation has encouraged researchers to develop another class of models, CZM, that is adaptive to these characteristics.

To overcome these limitations, advanced numerical models and experimental techniques have been developed, primarily within the CZM framework. These approaches aim to efficiently characterize both intrinsic and extrinsic energy dissipation.

Hu et al.[147] developed a general cohesive model that incorporates local crack propagation direction (see the definition of angles of fiber orientation and delamination direction in **Figure 15**a). The model has been implemented as a user element in FEM codes. The calculation of crack direction is based on the gradient of separation.[199] This enhancement enables consideration of the effect of crack propagation direction on delamination behavior, allowing relatively accurate prediction of complex delamination fronts with multiple delamination directions. By using this model, a relatively accurate prediction for complex delamination process, where the delamination initiating from the corner of a squared lamination, see Figure 15b, has been achieved. Good agreements have been observed for both the force displacement responses, see Figure 15c, and the delamination front configuration, see the comparison between Figure 15d,e.

Though the explicit description of the physical bridging can be a good approach to modeling the extrinsic dissipating events, the relatively complicated implementation and tailoring process for every specific application scenario makes the model unsuitable for broad applications. Considering this and to further account for the effect of FPZ length scale accurately, Li et al.[198] formulated the apparent delamination toughness of FRP as a function of multiple physical influencing factors, i.e., fiber orientation mismatch, delamination direction, width of crack front and depth of the LSB.

A global tracking scheme for delamination modeling is developed to quantify the multiple mechanisms influencing extrinsic dissipation. The model, incorporating the non-local dissipation mechanisms of delamination, excels in handling the most challenging delamination scenarios, where the delamination directions vary throughout the samples, and the delamination front evolves continuously.

5.2. Impact of Spatial Heterogeneities on Bridging

The spatial heterogeneity of interface properties may result in the bifurcation of the crack path within the interphase, which can be the root of the formation of fiber bridging in FRP or ligament bridging in secondary bonded joints. Understanding and controlling the spatial heterogeneity of interface properties are crucial for optimizing the performance and reliability of composite materials and bonded joints in various engineering applications. Advanced characterization techniques and computational modeling are often employed to study and predict the behavior of interfaces under different loading conditions.

Ashcroft et al.[200,201] applied a stochastic CZM to reproduce the scattering delamination response due to the effect of microstructural randomness. The relatively simple treatment of

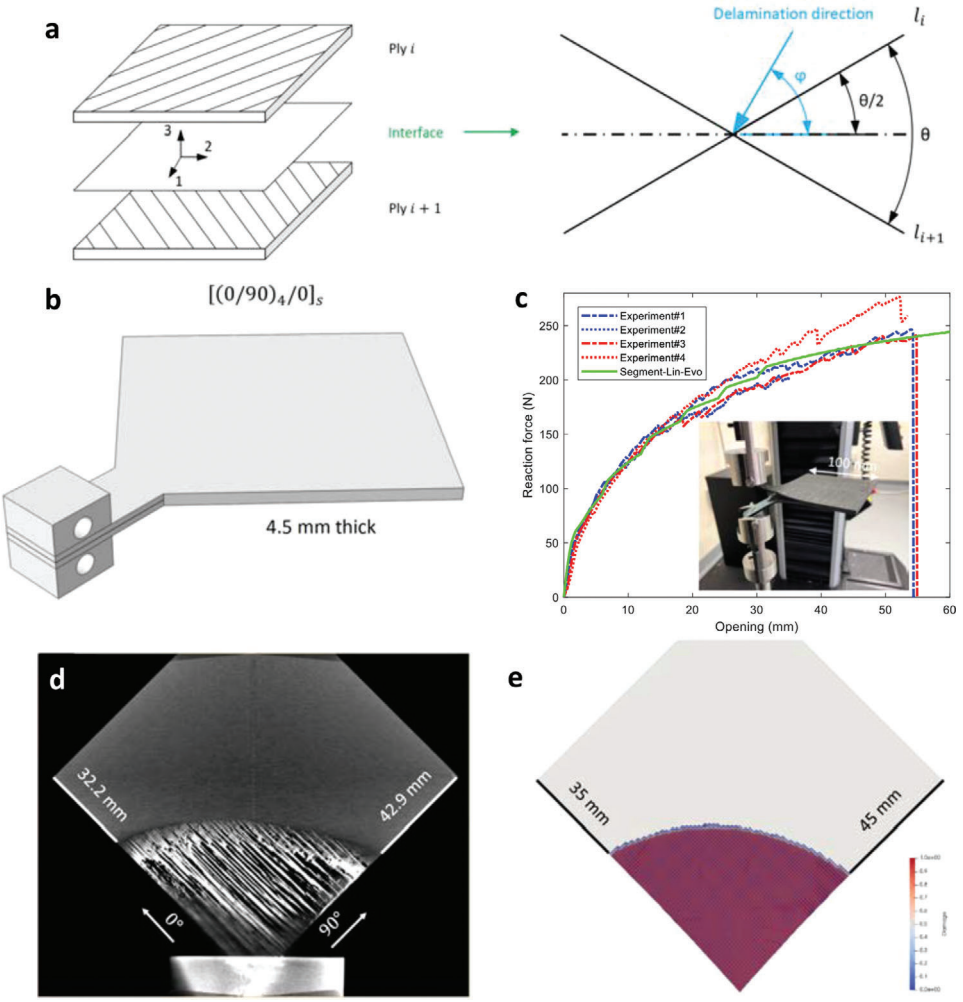

Figure 15. a) Definition of angles of fiber orientation and delamination direction. b) Geometry of the square sample for the Mode I fracture test. c) Comparison of the reaction-force-opening curve between experiments and simulations. Comparison of the delamination area between the experiments d) and simulation e) at the opening of 35 mm. Reproduced under the terms of the CC-BY Creative Commons Attribution 4.0 International license (https://creativecommons.org/licenses/by/4.0).[147] Copyright 2023, The Authors, published by Elsevier B.V.

the interphase of composites neglected the existence of fiber bridging and thus provided less reliable predictions.

To accurately characterize the effect of fiber bridging on the delamination response of laminated structures, a multiscale model based on CZM has been developed by Canal et al.[134,202] where an embedded cell approach was adopted to explicitly describe the large-scale bridging during delamination, in which fibers represented by beam elements, and connector elements with strength following a Weibull distribution are employed for linking the DCB arms and fibers. Thus, instead of using cohesive elements, decohesion behavior was represented by the connector failure and the current fiber bridging formed by pulling out of fibers. Using the same model, Hu et al.[100] investigated the influence of curing processes on the development of fiber bridging during delamination, highlighting the role of variance of fiber/matrix toughness in generating fiber bridging and probing the possible reason for the curing process effect on the delamination response of FRP. The embedded cell approach was recently applied to replicate the global force-displacement response when a DCB adhesive bonded joint is with ligament bridging.[203] Rafiee et al.[204] developed a multiscale framework for stochastic modeling for delamination of laminated composites containing CNTs. The stochastic multi-scale modeling procedure encompasses the integration of randomness to account for manufacturing-induced inconsistencies, treating variables such as CNT lengths, agglomeration, waviness patterns, and orientations as probabilistic entities, thus facilitating a comprehensive approach to modeling.

Similar to fiber bridging in FRP, secondary bonded joints may also form adhesive ligaments during the fracture process due to the spatial heterogeneity of adhesion.[14] These portions of the adhesive material bridge the crack, providing resistance to crack propagation and enhancing the strength and durability of the bonded joint.[205] Xu et al.[206] developed a numerical method using CZM modified by a user-defined subroutine to realize the randomly distributed adhesive properties. The bondline is treated as one single layer of CZM elements with randomly distributed properties, leading to a stochastic debonding process of adhesive joints. However, this model does not allow the

formation of ligaments, excluding the energy dissipation from the deformation of adhesives, while the contribution should not be neglected.

Inspired by the crack jumping across interfaces exhibited in a natural composite (the bark of a coconut tree), Sills and Thouless[207] considered strength discrepancy of interface in parallel cohesive zones and mimicked the phenomenon that the crack jumped from its original interface to the secondary interface with appropriate discrepancy subjected to a specific cohesive-length scale. They suggested that large-scale ligament bridging is a promising mechanism to be explored for toughening joints or materials.

By using a similar tool, Puspaningtyas et al.[208] proved the concept of tailoring the high-performance adhesive using microstructures exhibiting a negative Poisson's ratio to enhance the adhesion performance of single lap joints.

To investigate further how the random heterogeneity of adhesion improves the performance of composite bonded joints, Li et al. developed a model,[209,210] in which multiple cohesive elements are inserted surrounding the adhesive, which is modeled as elastoplastic material. The properties of the CZM are stochastic and follow a Gaussian process. Monte Carlo simulations are performed to achieve reliable statistical analysis. Results showed that, with the random variability of the interfacial properties, adhesive ligaments are formed during the delamination, which has significantly boosted the extrinsic dissipation and resulted in a high apparent fracture toughness. To investigate the effect of tailored defects on the delamination resistance of composite, Herraez et al.[211] adopted a similar concept of modeling with multiple interfaces to trigger bridging, which has successfully reproduced the phenomenon of multiple crack propagation, and the effective fracture resistance of the process. It should be mentioned here all these modeling approaches need to incorporate compensation of energy with viscous dissipation. This inclusion helps prevent non-convergence due to snapback instability when bridging is exerted during delamination.[212]

6. Applications of Extrinsic Toughening Concepts

6.1. Pressure Sensitive Tapes

Pressure Sensitive Adhesives (PSAs) are a category of thermoplastic adhesives with high tackiness that form strong bonds with substrates at room temperature, under low pressure, without the need for heat, hardeners, or catalysts.[213–215] This characteristic, which eliminates the necessity for chemical reactions during bonding, makes PSAs particularly appealing for various applications, including medical, automotive, home decoration, and sealing.[216]

Wagih et al. employed the sacrificial cracks technique, detailed in Section 4.2.1, to enhance the toughness, strength, and fatigue lifetime of PSAs.[217,218] The proposed method involved placing PTFE strips alternately over the upper and lower adhesive-liner interfaces. The modified PSAs exhibited significantly improved static and fatigue lap-shear strength and toughness compared to a baseline tape made from the same materials. The enhancements in strength and toughness were attributed to localized deformation at the defect sites, such that a portion of the applied energy was stored as elastic energy and withdrawn from the fracture process, thereby delaying interfacial debonding at the adhesive-substrate interface. After debonding initiation, the joint can sustain stresses due to partial stress release as local deformation at the defect sites until reaching ultimate strength. Even with the propagation of delamination at the adhesive-substrate interface, the formation of adhesive ligaments allowed the joint to sustain higher stress levels by distributing the load across the interfaces.[217] Experimental results indicated that these advanced tapes could withstand up to 83% and 210% increases in lap-shear strength and failure initiation strain, respectively, compared to conventional tapes.[217] It is emphasized that defect topology at the adhesive-carrier interface significantly affects the technique's efficiency. As shown in **Figure 16**, smaller defect sizes resulted in higher strain at equivalent defect ratios. Moreover, the advanced tapes demonstrated superior cyclic lap-shear performance. The defects facilitated the storage of applied energy as elastic deformation at the adhesive-carrier interface under cyclic loading, which reduced stress concentration at the adhesive-substrate interface and slowed the degradation rate of joint stiffness. This capability resulted in an extended lifespan, with the advanced tapes lasting nearly three times longer than the conventional ones.[217]

6.2. Composite T-Joints

Recently, various extrinsic toughening strategies have been deployed to a select few composite specimens and semi-structural components. However, among these, T-joints stand out as essential elements that not only interconnect members at perpendicular angles but also facilitate the formation of intricate structures while efficiently distributing loads.[219] The pursuit of enhanced composite T-joints through engineered toughened interfaces has emerged as a particularly promising avenue. Engineered toughened interfaces entail the intentional modification of material interfaces to bolster toughness, strength, and fracture resistance. This approach, aimed at elevating the mechanical performance and durability of composite structures, has garnered significant attention.[220] By introducing tailored structures, compositions, or pre-treatments at the interface between composite layers or components, the potential arises to alleviate stress concentrations, enhance energy dissipation, and impede crack propagation within the joint region.[221]

Following this overview, the subsequent sections will explore specific strategies for enhancing composite T-joints. These strategies include laser-based pre-treatment, microstructuring the bond line, and structuring the substrate/stiffener. Each of these techniques aims to further improve the mechanical performance and durability of composite structures by refining the interfaces and mitigating stress concentrations.

6.2.1. Laser-Based Pretreatment

Hashem et al.[222] demonstrated the efficiency of laser surface treatment of the skin and the stiffener surface on the improvement of strength and toughness of T-joints. Two different strategies were applied. The initial approach involved uniformly treating (cleaning) the skin and stiffener surfaces with laser treatment. The second approach entails alternating between high-power (ablation) and low-power (cleaning) laser irradiation on

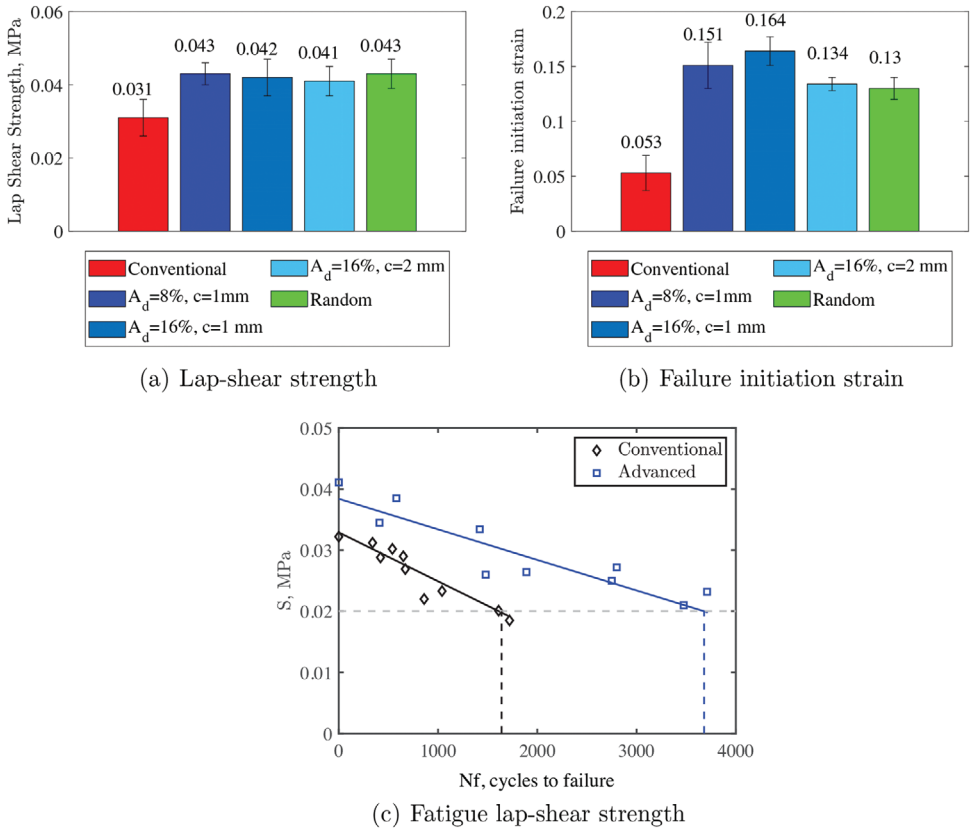

Figure 16. Lap-shear response of the advanced tapes (modified with sacrificial cracks): a) static strength, b) static failure initiation strain, and c) fatigue life. In a and b, A_d refers to the defect ratio with respect to the total area of adhesion and c refers to the defect width. Reproduced with permission.[217] Copyright 2024, Elsevier B.V.

these surfaces, creating a patterned surface through laser treatment (see **Figure** 17a). For a baseline joint (peel-ply treatment), a sudden load drop occurs suggesting a brittle failure, with an average maximum load of 788 ± 60 N as shown in Figure 17b. On the other hand, the laser-pretreated T-joint samples experienced progressive failure with numerous load drops before complete failure. The laser-cleaned samples that experienced low laser fluency demonstrated fewer load drops and failed at an average load of 1162 ± 91. The higher fluence ablated specimens had larger load drops and failed at an average load of 1314 ± 146 N.[222] The crack propagation and failure mode have been mainly affected by the laser surface pretreatment. For the baseline peel ply, pure interfacial failure was exhibited, with the crack propagation at the skin-adhesive interface. The load on the peel-ply joint steadily rose as the extension increased, reaching a peak before abruptly dropping at a minimal extension of 4 mm as shown in Figure 17. The laser pretreatment activated both interfacial and cohesive mechanisms, resulting in better load-displacement and toughness responses. The toughness of the T-joints improved by 2.8 times with laser cleaning, 5.0 times with laser ablation, and 12.0 times with laser patterning as compared to the baselines peel ply T-joints. During the pull-off test, damage emerged at the interfaces of the joint, propagating through a combination of mode I (opening) and mode II (shear) fractures.[223,224] More precisely, in the pull-off test conducted on the simply supported skin, notable bending deformations were evident at the midspan length. It was observed that crack propagation was mainly influenced by the fracture toughness of mode II rather than mode I.[225] Consequently, the predominant crack propagation mode in this study was identified as mode II (shear mode). The low toughness of untreated surfaces is due to contaminants present on the surface which reduce bonding between the skin and the adhesive, decreasing both mode I and II fracture toughness and resulting in premature joint failure. Additionally, the rough surface texture hindered bonding, particularly at surface dents. In contrast, the laser-cleaned joint experienced improved bonding due to contaminant removal and slight surface texture modification. This enhanced interface bonding increased interface toughness more than adhesive toughness, allowing cracks to propagate within the adhesive layer, resulting in cohesive failure.[222]

Unlike the untreated joints, where a brittle failure occurs due to the fast propagation of a crack at the adhesive-skin interface, the laser-patterned joint demonstrated progressive damage mode as shown in Figure 17d. Initially, slight load drops occurred before damage initiation at the stiffener/adhesive interface in the delta fillet region. Subsequently, crack propagation ensued until reaching the laser-cleaned treated area, where the crack was halted due to roughness differences between ablated and cleaned areas. A load drop occurred as the crack migrated to the skin/adhesive interface, leading to adhesive layer breakage. The load then increased without crack propagation, as the laser cleaning treatment arrested the crack. When energy exceeded the

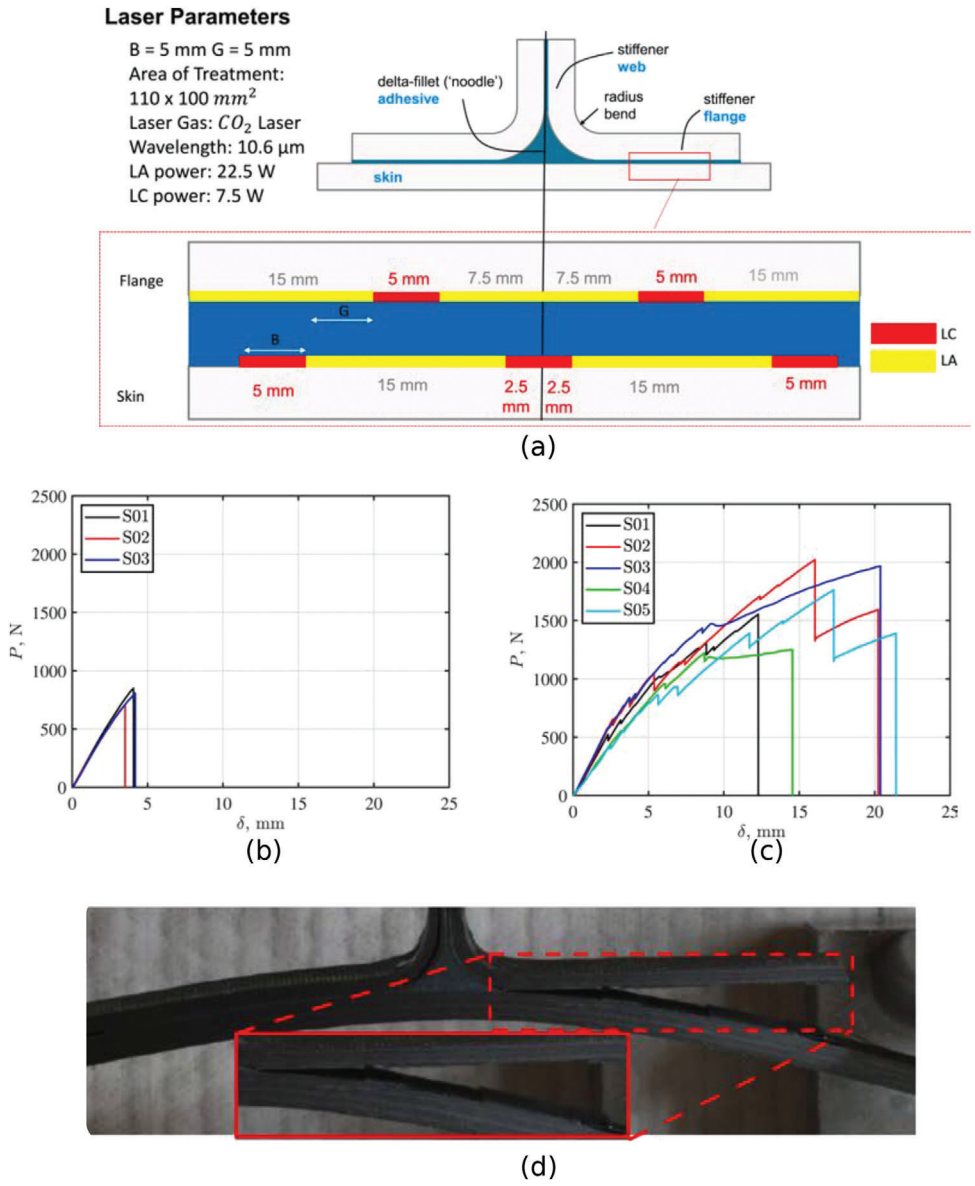

Figure 17. Pull off test results of T-joints: a) $P-\delta$ curve of Baseline PeelPly T-joints. b) $P-\delta$ curve of Novel Laser Patterned T-joints. c) In situ progressive damage ligaments in laser patterned T-joint from laser patterned T-joints. Reproduced with permission.[222] Copyright 2022, Elsevier B.V.

joint's limit, high localized stresses caused a second crack initiation at the skin/adhesive interface end. This crack propagated until reaching the laser-cleaned treatment layer on the skin, where it was arrested and then extended to the stiffener/adhesive interface, forming an adhesive ligament.

6.2.2. Microstructuring of Adhesive Bondline

The concept of hierarchical design principles, inspired by biological structures, was applied at multiple levels to develop an innovative CFRP T-joint with enhanced structural characteristics, potentially suitable for lightweight aircraft structures. Wagih et al.[226] proposed a bio-inspired T-joint, where sacrificial cracks (method described in Section 4.2.1) were embedded at the adhesive bondline to enhance the toughness and strength of the joint. In this method, the sacrificial cracks was embedded to allow crack migration between the upper and lower adhesive–adherend interfaces that forms an adhesive ligament. The formation of this ligament allows for dissipation of energy by the propagation of larger surface crack area at the upper and lower interface and plastic deformation of the ligament. The effect of four different adhesive thicknesses, 0.3, 0.5, 0.8, and 1.0 mm, respectively, have been studied in both conventional and bioinspired T-joints. Pull-off tests have been conducted, and the conventional T-joints demonstrated sudden brittle failure, while the bioinspired T-joints showed progressive failure. The energy dissipation in the bioinspired joints with thin (0.3 and 0.5 mm) adhesive was 3.3 times greater than that observed in the conventional joint. The behavior of conventional T-joints with thicker

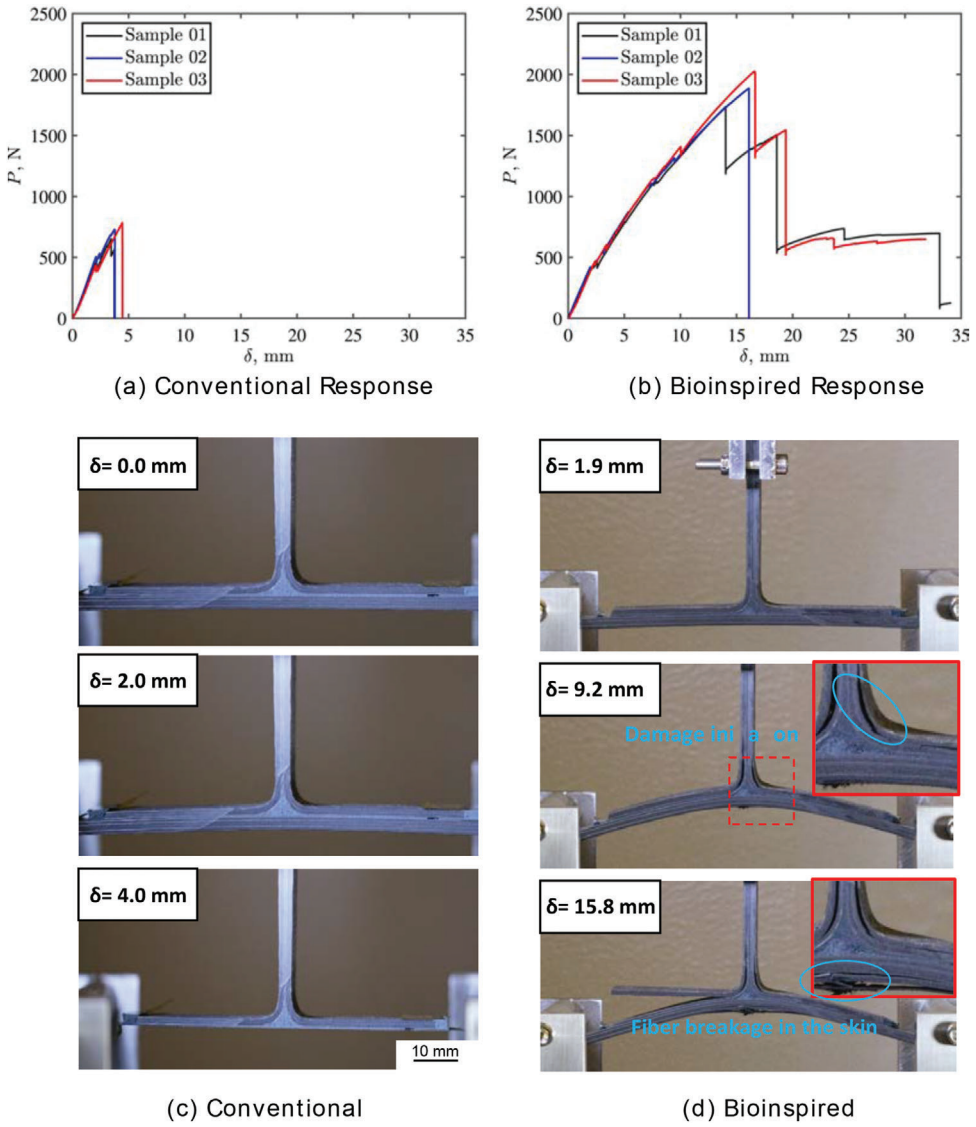

Figure 18. Damage evolution in the thick adhesive bioinspired T-joint (1.0 mm). Reproduced with permission.[226] Copyright 2022, Elsevier B.V.

adhesive layers (0.8 and 1.0 mm) was similar to those of conventional T-joints with thinner adhesive layers. However, when it came to bioinspired T-joints the increase in thickness played an important role in improving energy dissipation and toughness. **Figure 18** shows the load-displacement responses and the associated damage modes at different loading stages, highlighting a sudden load drop at an early loading stage, around 4 mm, for the conventional joint. The sudden load drop and complete failure were due to the complete separation at the skin–adhesive interface. However, for the bioinspired joint, the joint was able to sustain larger deformation reaching 15 mm, without failure due to the presence of the sacrificial cracks in the interface that enhanced the toughness of the skin–stiffener interface. Unlike the conventional joint, a progressive damage mode was observed for this joint, where the damage initiated at the corner of the stiffener and propagated at this position. Increasing the displacement, the damage initiated inside the skin and between the stiffener plies. This progressive distributed damage inhibited the complete failure of the joint even at high deformation.

6.2.3. Substrate/Stiffener Structuring

Morano et al[227] proposed a new design approach to improve the toughness of the adhesive bonded metal-composite T-joints by tailoring the metal stiffener via incorporating grooves (i.e., corrugation) along the unbounded surface of the metal stiffener as illustrated in **Figure 19a**. As shown in the previous section, tailoring the architecture of the mating layers facilitates stress redistribution at the bondline, thereby delaying damage initiation and ultimately improving toughness. The results of the pull-off test for the base and the corrugated T-joints showed a significant increase in the pull-off strength and absorbed energy reached up to 65%, and 416%, respectively, for the corrugated

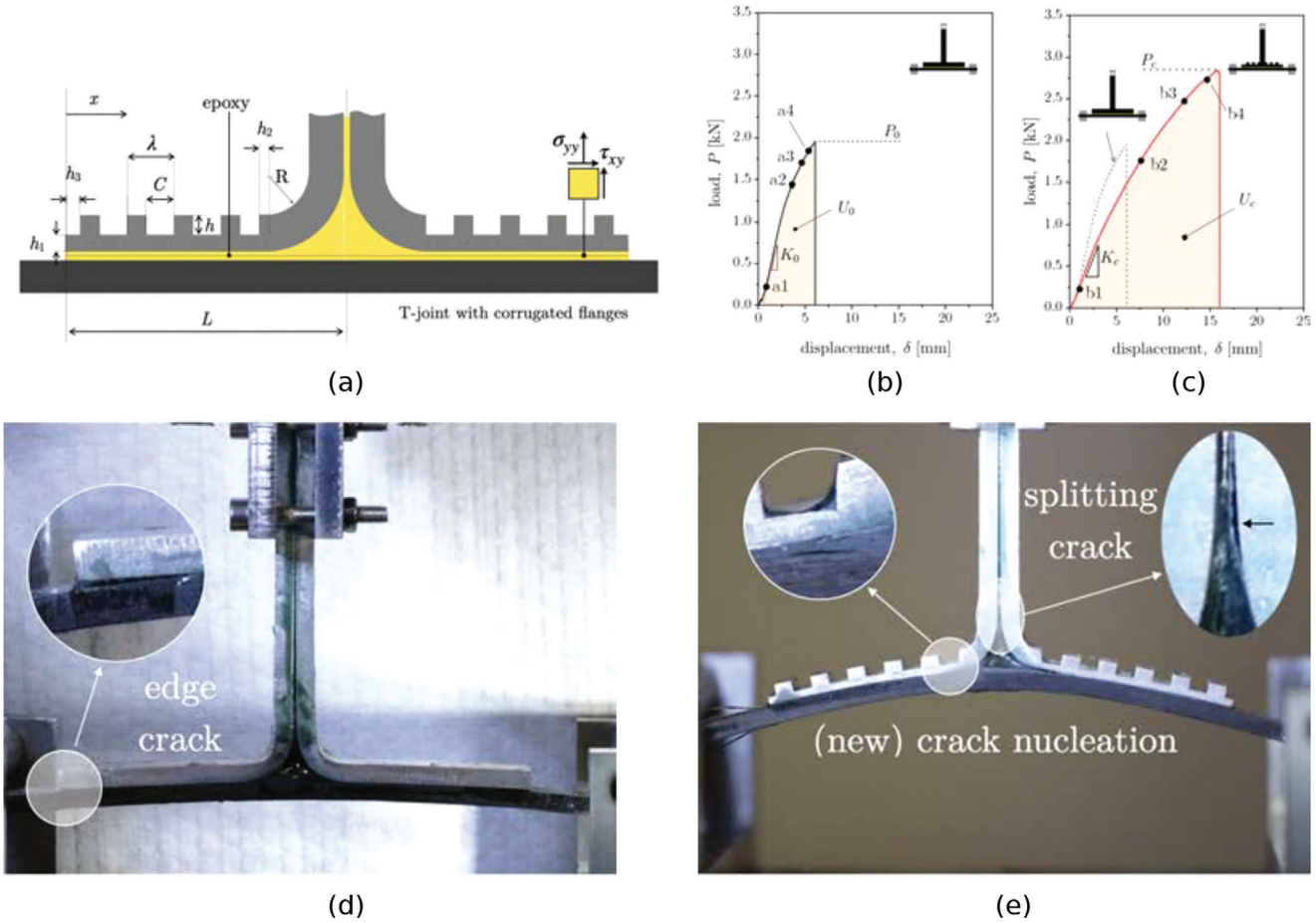

Figure 19. a) Schematic of the Corrugated Aluminum Stiffener. b,c) Pull-off response of base and corrugated T-joints respectively. d,e) show the damage initiation locations in the base and the corrugated T-joints respectively. Reproduced with permission. Copyright 2023, Elsevier B.V.

T-joints compared to a baseline joint of the same material and thickness as presented in Figure 19b,c.

By investigating the damage modes in the baseline and corrugated T-joints reported in Figure 19d,e, it was noted that in the baseline joint, the crack initiated at the edge of the interface between CFRP skin and metal stiffener due to the high-stress concentration at the edge. While, in the case of corrugated aluminum stiffener, the damage began at the stiffener/skin interface under the first groove. Using the corrugated pattern leads to redistribution of the stress along the bondline and moves the crack initiation from the free edge to start under the first groove near the delta region, which leads to retarding in crack propagation and increasing the joint toughness.

Still in this area, Wagih et al.[228] introduced a similar method to enhance the toughness of hybrid metal-composites T-joints by 3D printing the metal stiffener in an auxetic shape. This study used a selective laser melting technique to print a stainless steel stiffener with a re-entrant structure, as shown in **Figure 20**a. They compared three configurations: one base model and two auxetic structures with different sizes of the re-entrant structure as illustrated in Figure 20a. A pull-off test was performed to characterize the toughness and strength of the fabricated T-joints. As shown in Figure 20c–e. They reported that using auxetic structures reflected in a significant improvement in the strength of the one-row and two-row auxetic structures compared to the base joint, achieving 2.7, 2.1 times, respectively, as reported in Figure 20b,c,d). Additionally, the toughness of these joints enhanced dramatically to reach 60 and 31.8 times for one and two rows of auxetic structures, respectively, compared to the base joint. This outstanding performance was due to retarding the delamination between the metal stiffener and CFRP skin that occurred by changing the localized bending stiffness at the transition position between the re-entrant structures and the bulk web. The damage initiation and propagation for each configuration were reported as presented in Figure 20e,f,g. Whereas in the base joint (Figure 20e), the damage started at the early loading stage and initiated at the edge of the T-joint due to the high-stress concentration, then continued in propagation by increasing the applied displacement. While in the case of auxetic structures, the damage initiation was retarded compared to the base joint. Unlike the base joint, the damage in Auxetic #1 and Auxetic #2 started in the interface between the CFRP skin and the metal stiffener under the transition between the bulk web and the re-entrant structures as shown in Figure 20f,e.

The innovative methods discussed for enhancing the toughness of adhesive-bonded metal-composite T-joints emphasize the critical role of interface engineering and structural modifications.

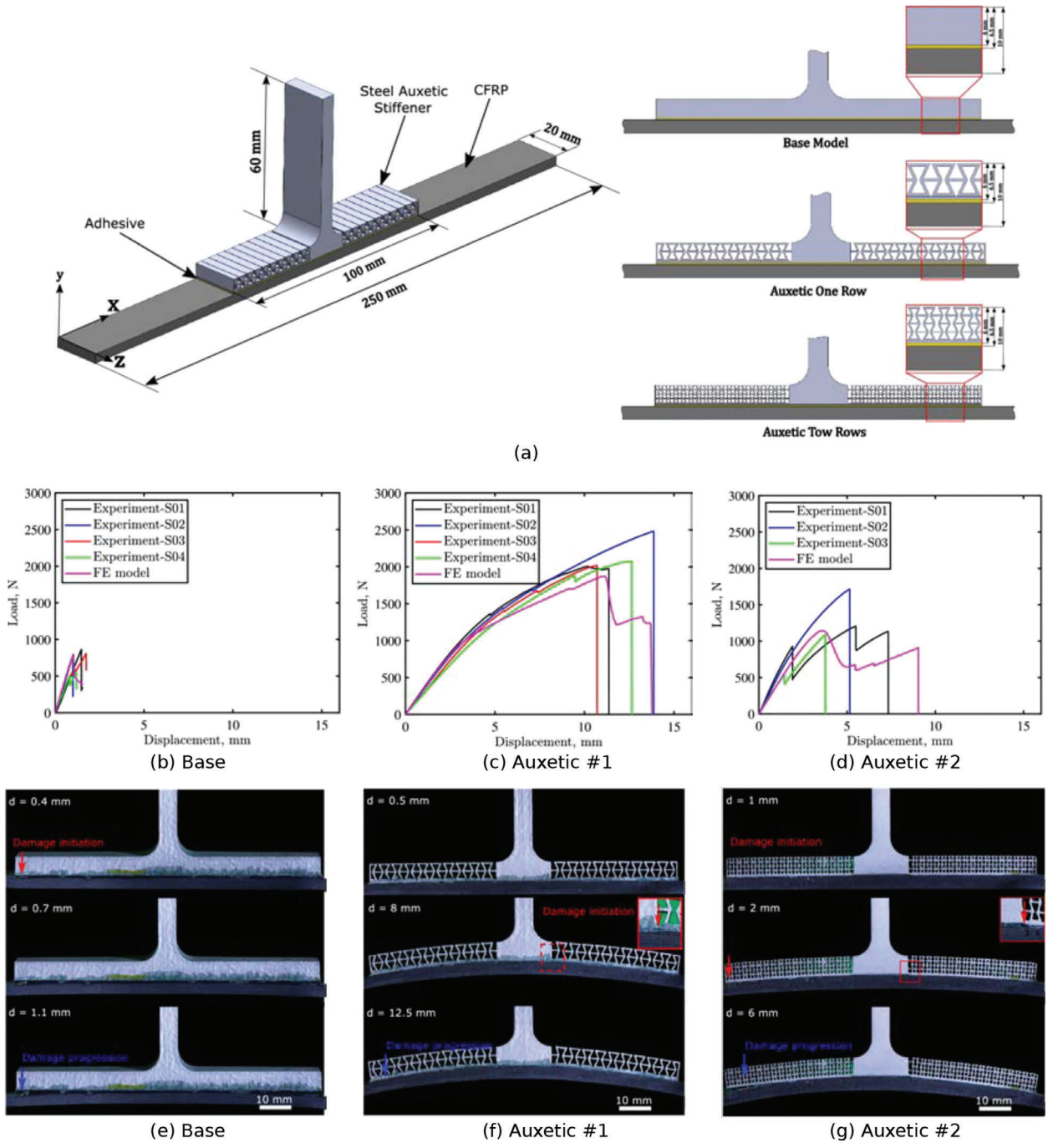

Figure 20. a) Schematic illustration of auxetic metal-composites T-joint. b,c) and d) Response of pull-off test of different configurations. e,f), and g) Damage initiation and propagation in tested configurations. Reproduced with permission.[228] Copyright 2024, Elsevier B.V.

Techniques such as corrugating the metal stiffener and 3D printing auxetic structures have shown substantial improvements in the mechanical performance of T-joints by redistributing stress and delaying crack initiation. These advancements highlight the potential of tailored design approaches to significantly enhance the strength and durability of composite structures. Future research should continue to investigate and optimize these strategies, integrating them with emerging technologies to further improve the performance and reliability of composite assemblies in various applications.

7. Concluding Remarks and Future Challenges

Throughout this review, we have demonstrated how the extrinsic component of dissipation can be strategically manipulated through carefully designed microstructures to achieve

exceptional properties. While classical fracture mechanics typically enhance performance by reducing stress concentrations or lowering energy release rates during crack propagation (i.e., the driving force of failure), the approaches discussed in this review differ significantly. They aim to optimize energy dissipation throughout the material's bulk. Whether through promoting bridging or bulk dissipation (within either the bondline or the adherends), these strategies aim to transform surface dissipation, which is inherently limited as it operates only on a material plane, into volume dissipation.

We have also highlighted how customizing the architecture of the mating layers enhances the mechanical performance of laminated structures. By precisely adjusting the geometrical properties of subsurface regions adjacent to the interface, laminates can be strengthened, allowing for enhanced energy dissipation without altering key joint attributes like the interface or bondline composition. The toughening effects observed suggest that architected materials can be precisely engineered to control crack propagation behavior. This finding is not only theoretically interesting but also has practical implications, such as cases where cracks growth along weaker planes. Additionally, the numerical analysis revealed that the pattern shape in the architected region affects crack behavior, opening the door to optimization (for example driven by machine learning methods) for further applications.

A key strength of these methods is that exceptional performance can be achieved without altering the constitutive material itself. In theory, any material can be toughened using the techniques showcased in this review. This is crucial because, for many applications, material choice is often constrained by other considerations. This is especially true in the healthcare sector, where introducing new materials is extremely challenging. Using materials that are already qualified and recognized as biocompatible and non-toxic can accelerate the development process. The potential for advancement in this area is further enhanced when these methods are used in conjunction with additive manufacturing. New additive manufacturing technologies allow for the design of fine microstructures with heterogeneous and high-contrast material properties. The strategies presented here can be applied to toughen 3D-printed parts and improve their mechanical performance. This is particularly important, as the mechanical performance of 3D-printed parts currently lags behind that of parts produced by traditional manufacturing techniques.

Despite the promising results, several gaps and challenges remain in fully harnessing these dissipation mechanisms. A significant gap is the ability to effectively deploy and control bridging within the material microstructure. While strategies to promote bridging have been identified, there is still limited understanding of how to precisely control this mechanism to maximize extrinsic dissipation without compromising other critical properties, such as stiffness or in-plane strength. This lack of understanding and control hinders the ability to tailor extrinsic dissipation mechanisms to meet specific engineering requirements effectively. Additionally, the scalability of these strategies to various types of composites and adhesive bonds is not yet fully understood. The effectiveness of extrinsic dissipation mechanisms may vary significantly depending on the material system, processing conditions, and loading scenarios. More systematic studies are needed to determine how these factors influence the performance of designed microstructures and to identify the conditions under which these strategies can be most effectively applied.

Furthermore, extrinsic effects can lead to significant changes in fracture properties, particularly in toughness, which may vary greatly depending on the extent of non-local mechanisms such as bridging. Modeling these effects is challenging, as it requires non-local approaches that account for the complex interactions between the structure's kinematics and the material's response at a detailed level. Although recent efforts documented in this paper have advanced in this area, substantial gaps remain. Traditional local continuum models often fall short in representing non-local effects because they do not account for interactions beyond the immediate vicinity of the crack tip. Consequently, they may oversimplify or overlook critical contributions from mechanisms that operate over larger spatial scales. There is a need for more sophisticated computational methods to handle the increased complexity introduced by extrinsic dissipation mechanisms. As discussed in this review, progress has been made in modeling extrinsic dissipation, but more advanced, multi-scale, and computationally efficient models are needed to accurately predict the complex fracture behavior of composites and adhesive bonds, including phenomena such as snap-back and snap-through instabilities observed in experiments. Addressing these gaps will be crucial for developing more reliable and robust design tools for engineering applications where fracture resistance is a critical concern.

In summary, while the strategies for leveraging extrinsic dissipation show significant promise, there are still important gaps that must be addressed to fully realize their potential. Addressing these challenges will be crucial for advancing the design of tough, high-performance materials across a range of applications and for ensuring that these innovations can be successfully implemented in real-world engineering systems.

Acknowledgements

This research was supported by King Abdullah University of Science and Technology (KAUST) under award numbers BAS/1/1315-01-01 and OSR-2017-CRG6-3388.01 and the IAF project number: REI/1/5134-01-01.

Conflict of Interest

The authors declare no conflict of interest.

Keywords

adhesive bonding, CFRP, delamination, interface, toughening

Received: May 19, 2024
Revised: October 22, 2024
Published online: November 20, 2024

[1] J. Prunier, M. Cahen, *JEC Composites Magazine* **2024**, *158*, 17.
[2] CompositesWorld, Composites End Markets: Automotive (2024), **2024**.
[3] MC: Advanced Materials, Report Code: A09125, Pages: 710, **2024**.

[4] F. Khan, N. Hossain, J. J. Mim, S. M. Rahman, M. J. Iqbal, M. Billah, M. A. Chowdhury, *J. Eng. Res.* **2024**, in Press.
[5] JEC Observer: Current trends in the global composites industry 2022-2027, *JEC Publications* (**2023**).
[6] Y. Ou, C. Gonzalez, J. J. Vilatela, *Composites, Part B* **2020**, *201*, 108372.
[7] Y. Ou, L. Wu, M. Hefetz, C. Gonzalez, J. Jose Vilatela, *Composites, Part A* **2023**, *164*, 107283.
[8] A. Mouritz, *Composites, Part A* **2007**, *38*, 2383.
[9] H. An, B. D. Youn, H. S. Kim, *Int. J. Mech. Sci.* **2021**, *205*.
[10] E. Garcia, B. Wardle, A. John Hart, *Composites, Part A* **2008**, *39*, 1065.
[11] S. Wicks, R. de Villoria, B. Wardle, *Compos. Sci. Technol.* **2010**, *70*, 20.
[12] X. Ni, C. Furtado, N. Fritz, R. Kopp, P. Camanho, B. Wardle, *Compos. Sci. Technol.* **2020**, *190*.
[13] J. Kupski, S. T. de Freitas, *Compos. Struct.* **2021**, *268*, 113923.
[14] R. Tao, M. Alfano, G. Lubineau, *Composites, Part A* **2018**, *109*, 84.
[15] A. Yudhanto, M. Alfano, G. Lubineau, *Composites, Part A* **2021**, *147*, 106443.
[16] P. Ladeveze, G. Lubineau, D. Marsal, *Compos. Sci. Technol.* **2006**, *66*, 698.
[17] R. Khan, *Compos. Struct.* **2019**, *229*, 111418.
[18] Y. Wu, Y. Gong, D. Tian, L. Zou, L. Zhao, J. Zhang, N. Hu, *Compos. Struct.* **2023**, *322*, 117345.
[19] L. Canal, M. Alfano, J. Botsis, *Compos. Sci. Technol.* **2017**, *139*, 90.
[20] E. Farmand-Ashtiani, J. Cugnoni, J. Botsis, *Int. J. Solids Struct.* **2015**, *55*, 58.
[21] A. C. Orifici, P. Wongwichit, N. Wiwatanawongsa, *Composites, Part A* **2014**, *66*, 218.
[22] M. Herráez, N. Pichler, J. Botsis, *Compos. Struct.* **2020**, *247*, 112422.
[23] R. Tao, X. Li, A. Yudhanto, M. Alfano, G. Lubineau, *Compos. Sci. Technol.* **2020**, *188*, 107964.
[24] A. Yudhanto, M. Almulhim, F. Kamal, R. Tao, L. Fatta, M. Alfano, G. Lubineau, *Compos. Sci. Technol.* **2020**, *199*, 108346.
[25] R. Tao, X. Li, A. Yudhanto, M. Alfano, G. Lubineau, *Composites, Part A* **2022**, *158*, 106954.
[26] T.-H. Jiang, Z.-G. Yang, *Engineering Failure Analysis* **2024**, *160*, 108233.
[27] B. Manshadi, E. Farmand-Ashtiani, J. Botsis, A. Vassilopoulos, *Composites, Part A* **2014**, *61*, 43.
[28] S. Heide-Jørgensen, S. Teixeira de Freitas, M. Budzik, *Compos. Sci. Technol.* **2018**, *160*, 97.
[29] T. Zhu, Z. Ren, J. Xu, L. Shen, C. Xiao, C. Zhang, X. Zhou, X. Jian, *Compos. Sci. Technol.* **2023**, *244*, 110300.
[30] R. Lima, R. Tao, A. Bernasconi, M. Carboni, N. Carrere, S. Teixeira de Freitas, *Composites, Part B* **2023**, *263*, 110853.
[31] L. P. Canal, C. Gonzalez, J. Segurado, J. LLorca, *Compos. Sci. Technol.* **2012**, *72*, 1223.
[32] M. Wisnom, *Philos. Trans. Roy. Soc. A: Math. Phys. Eng. Sci.* **2012**, *370*, 1850.
[33] W. Tu, J.-A. Pascoe, R. Alderliesten, *Compos. Struct.* **2024**, *339*, 118137.
[34] J. C. Brewer, P. A. Lagace, *J. Compos. Mater.* **1988**, *22*, 1141.
[35] J. Wang, W. Chang, M. S. Islam, F. Huang, S. Wu, L. F. Rose, J. Zhang, C. H. Wang, *Compos. Sci. Technol.* **2024**, *251*, 110548.
[36] K. Dransfield, C. Baillie, Y.-W. Mai, *Compos. Sci. Technol.* **1994**, *50*, 305.
[37] T. Sebaey, N. Blanco, J. Costa, C. Lopes, *Compos. Sci. Technol.* **2012**, *72*, 1251.
[38] J. Rzeczkowski, S. Samborski, M. de Moura, *Materials* **2020**, *13*, 5146.
[39] J. Gonzalez-Cantero, E. Graciani, B. Lopez-Romano, F. Paris, *Compos. Sci. Technol.* **2018**, *156*, 223.
[40] Y. Li, B. Wang, L. Zhou, *Eng. Fail. Anal.* **2023**, *153*, 107576.
[41] W. Wu, S. Li, X. Qin, G. Fu, Z. Bao, H. Li, Q. Zhao, *J. Mater. Res. Technol.* **2024**, *30*, 3052.
[42] Y. Gao, L. Shi, T. Lu, W. Xie, X. Cai, *Eng. Fract. Mech.* **2024**, *295*, 109797.
[43] S. Onodera, K. Kawahara, S. Yashiro, *Eng. Fract. Mech.* **2023**, *293*, 109681.
[44] D. Kim, C. Hong, *Compos. Sci. Technol.* **1992**, *43*, 147.
[45] ASTM d5528: Standard test method for mode I interlaminar fracture toughness of unidirectional fiber-reinforced polymer matrix composites, **2013**.
[46] ASTM d7905: Standard test method for determination of the mode II interlaminar fracture toughness of unidirectional fiber-reinforced polymer matrix composites using the end-notched flexure (ENF) test, **2014**.
[47] X. Li, G. Lubineau, *J. Mech. Phys. Solids* **2024**, 105795.
[48] C. Audd, B. D. Davidson, J. G. Ratcliffe, M. W. Czabaj, *Eng. Fract. Mech.* **2019**, *215*, 138.
[49] ASTM International, Standard test method for mixed mode I-mode II interlaminar fracture toughness of unidirectional fiber reinforced polymer matrix composites, ASTM D6671, **2023**.
[50] E. Farmand-Ashtiani, J. Cugnoni, J. Botsis, *Int. J. Solids Struct.* **2015**, *55*, 58.
[51] G. Frossard, J. Cugnoni, T. Gmür, J. Botsis, *Composites, Part A* **2016**, *91*, 1.
[52] E. Farmand-Ashtiani, J. Cugnoni, J. Botsis, *Compos. Sci. Technol.* **2016**, *137*, 52.
[53] M. Herráez, N. Pichler, G. Pappas, C. Blondeau, J. Botsis, *Composites, Part A* **2020**, *134*, 105886.
[54] N. Pichler, M. Herráez, J. Botsis, *Composites, Part B* **2020**, *197*, 108089.
[55] C. Blondeau, G. Pappas, J. Botsis, *Compos. Struct.* **2019**, *216*, 464.
[56] G. A. Pappas, J. Botsis, *Int. J. Solids Struct.* **2020**, *191*, 42.
[57] O. Allix, P. Ladeveze, *Arch. Mech.* **1992**, *44*, 5.
[58] R. de Borst, *Eng. Fract. Mech.* **2002**, *69*, 95.
[59] T. Rabczuk, *Int. Scholarly Res. Not.* **2013**, *2013*.
[60] Y. Sun, M. G. Edwards, B. Chen, C. Li, *Eng. Fract. Mech.* **2021**, *257*, 108036.
[61] J. Lemaitre, *Proceedings of International Conference of Mechanical Behavior of Materials*, **1971**.
[62] M. Wnuk, R. Kriz, *Int. J. Fract.* **1985**, *28*, 121.
[63] J. Maire, J. Chaboche, *Aerospace Sci. Technol.* **1997**, *1*, 247.
[64] P. Maimí, P. P. Camanho, J. Mayugo, C. Dávila, *Mech. Mater.* **2007**, *39*, 897.
[65] X. Li, W. Gao, W. Liu, *Int. J. Damage Mech.* **2019**, *28*, 1299.
[66] G. A. Francfort, J.-J. Marigo, *J. Mech. Phys. Solids* **1998**, *46*, 1319.
[67] B. Bourdin, G. A. Francfort, J.-J. Marigo, *J. Mech. Phys. Solids* **2000**, *48*, 797.
[68] B. Bourdin, G. A. Francfort, J.-J. Marigo, *J. Elasticity* **2008**, *91*, 5.
[69] M. Ambati, T. Gerasimov, L. De Lorenzis, *Comput. Mech.* **2015**, *55*, 383.
[70] W. Tan, B. G. Falzon, L. N. Chiu, M. Price, *Composites, Part A* **2015**, *71*, 212.
[71] M. N. Saleh, G. Lubineau, P. Potluri, P. J. Withers, C. Soutis, *Compos. Struct.* **2016**, *156*, 115.
[72] O. Allix, L. Gornet, P. Ladevèze, D. Lévêque, *Proceedings of the IUTAM Symposium held in Paris, France*, Springer, Berlin, Germany **1999**, pp. 163–171.
[73] C. V. Verhoosel, R. de Borst, *Int. J. Numer. Meth. Eng.* **2013**, *96*, 43.
[74] B. Dhas, M. Masiur Rahaman, K. Akella, D. Roy, J. Reddy, *J. Appl. Mech.* **2018**, *85*, 011010.
[75] A. Quintanas-Corominas, A. Turon, J. Reinoso, E. Casoni, M. Paggi, J. Mayugo, *Comp. Meth. Appl. Mech. Eng.* **2020**, *358*, 112618.
[76] T. Q. Bui, X. Hu, *Eng. Fract. Mech.* **2021**, *248*, 107705.

[77] G. Li, B. Yin, L. Zhang, K. Liew, *Comp. Meth. Appl. Mech. Eng.* **2021**, *382*, 113872.
[78] G. R. Irwin, *J. Appl. Mech.* **1957**, *24*, 361.
[79] R. Krueger, *Appl. Mech. Rev.* **2004**, *57*, 109.
[80] M. Benzeggagh, M. Kenane, *Compos. Sci. Technol.* **1996**, *56*, 439.
[81] P. P. Camanho, C. G. Dávila, Technical report, **2002**.
[82] J. R. Reeder, *American Society for composites 21st annual technical conference*, **2006**.
[83] M. Heidari-Rarani, M. Sayedain, *Theor. Appl. Fract. Mech.* **2019**, *103*, 102246.
[84] D. S. Dugdale, *J. Mech. Phys. Solids* **1960**, *8*, 100.
[85] G. Barenblatt, *Adv. Appl. Mech.* **1962**, *7*, 55.
[86] A. Needleman, *J. Mech. Phys. Solids* **1990**, *38*, 289.
[87] A. Tabiei, W. Zhang, *Appl. Mech. Rev.* **2018**, *70*, 030801.
[88] L. A. de Oliveira, M. V. Donadon, *Eng. Fract. Mech.* **2020**, *235*, 107124.
[89] G. Goldoni, S. Mantovani, *Compos. Struct.* **2021**, *275*, 114493.
[90] J. Cao, J. Gu, Z. Dang, C. Zhang, *Composites, Part A* **2023**, *171*, 107581.
[91] K. Park, G. H. Paulino, *Appl. Mech. Rev.* **2011**, *64*, 060802.
[92] P. P. Camanho, C. G. Davila, M. De Moura, *J. Compos. Mater.* **2003**, *37*, 1415.
[93] A. Cerrone, P. Wawrzynek, A. Nonn, G. H. Paulino, A. Ingraffea, *Eng. Fract. Mech.* **2014**, *120*, 26.
[94] M. Elices, G. Guinea, J. Gomez, J. Planas, *Eng. Fract. Mech.* **2002**, *69*, 137.
[95] Q. Yang, B. Cox, *Int. J. Fract.* **2005**, *133*, 107.
[96] H. Li, N. Chandra, *Int. J. Plast.* **2003**, *19*, 849.
[97] Q. Xu, Z. Lu, *Int. J. Plast.* **2013**, *41*, 147.
[98] L. A. de Oliveira, M. V. Donadon, *Eng. Fract. Mech.* **2020**, *228*, 106922.
[99] C. Sarrado, A. Turon, J. Renart, I. Urresti, *Compos., Part A* **2012**, *43*, 2128.
[100] P. Hu, D. Pulungan, R. Tao, G. Lubineau, *Compos., Part A* **2021**, *149*, 106564.
[101] P. Hu, R. Tao, X. Li, G. Lubineau, *Compos. Sci. Technol.* **2022**, *229*, 109684.
[102] Y. Lin, L. Freund, *Int. J. Solids Struct.* **2007**, *44*, 1927.
[103] H.-P. Zhao, Y. Wang, B.-W. Li, X.-Q. Feng, *Int. J. Appl. Mech.* **2013**, *5*, 1350012.
[104] L. Sorensen, J. Botsis, T. Gmür, J. Cugnoni, *Compos., Part A* **2007**, *38*, 2087.
[105] B. Blaysat, J. P. Hoefnagels, G. Lubineau, M. Alfano, M. G. Geers, *Int. J. Solids Struct.* **2015**, *55*, 79.
[106] L. Bouhala, A. Makradi, S. Belouettar, A. Younes, S. Natarajan, *Compos. Struct.* **2015**, *153*, 91.
[107] A. De Morais, A. Pereira, M. De Moura, F. Silva, N. Dourado, *Compos. Struct.* **2015**, *122*, 361.
[108] S. M. Jensen, M. Martos, E. Lindgaard, B. L. V. Bak, *Compos. Struct.* **2019**, *225*, 111074.
[109] A. Turon, C. G. Davila, P. P. Camanho, J. Costa, *Eng. Fract. Mech.* **2007**, *74*, 1665.
[110] A. Turon, P. Camanho, J. Costa, J. Renart, *Compos. Struct.* **2010**, *92*, 1857.
[111] X. Lu, M. Ridha, B. Chen, V. Tan, T. Tay, *Eng. Fract. Mech.* **2019**, *206*, 278.
[112] R. Branco, F. Antunes, J. Costa, *Eng. Fract. Mech.* **2015**, *141*, 170.
[113] N. Moës, J. Dolbow, T. Belytschko, *Int J. Num. Meth. Eng.* **1999**, *46*, 131.
[114] T. Belytschko, R. Gracie, *Int. J. Plast.* **2007**, *23*, 1721.
[115] R. de Borst, J. J. Remmers, *Compos. Sci. Technol.* **2006**, *66*, 713.
[116] S. Yazdani, W. J. Rust, P. Wriggers, *Compos. Struct.* **2016**, *135*, 353.
[117] L. Zhao, J. Zhi, J. Zhang, Z. Liu, N. Hu, *Compos. Part A* **2016**, *80*, 61.
[118] X. Li, J. Chen, *Compos. Struct.* **2016**, *143*, 1.
[119] N. Stein, S. Dölling, K. Chalkiadaki, W. Becker, P. Weißgraeber, *Int. J. Fract.* **2017**, *207*, 193.
[120] D. Grogan, C. Ó. Brádaigh, S. Leen, *Compos. Struct.* **2015**, *120*, 246.
[121] R. Higuchi, T. Okabe, T. Nagashima, *Compos. Part A* **2017**, *95*, 197.
[122] F. Teimouri, M. Heidari-Rarani, F. H. Aboutalebi, *Eng. Fract. Mech.* **2021**, *249*, 107760.
[123] M. Marulli, A. Valverde-González, A. Quintanas-Corominas, M. Paggi, J. Reinoso, *Comp. Meth. Appl. Mech. Eng.* **2022**, *395*, 115007.
[124] T.-P. Fries, *Pamm* **2014**, *14*, 27.
[125] E. Gordeliy, A. Peirce, *Comp. Meth. Appl. Mech. Eng.* **2015**, *283*, 474.
[126] G. Vigueras, F. Sket, C. Samaniego, L. Wu, L. Noels, D. Tjahjanto, E. Casoni, G. Houzeaux, A. Makradi, J. M. Molina-Aldareguia, M. Vázquez, A. Jérusalem, *Compos. Struct.* **2015**, *125*, 542.
[127] G. Lubineau, A. Rahaman, *Carbon* **2012**, *50*, 2377.
[128] C. S. Grimmer, C. Dharan, *Compos. Sci. Technol.* **2010**, *70*, 901.
[129] A. R. Ravindran, R. B. Ladani, S. Wu, A. J. Kinloch, C. H. Wang, A. P. Mouritz, *Compos. Sci. Technol.* **2018**, *167*, 115.
[130] Y. He, K. Duan, L. Yao, J. Tang, J. Zhang, D. Jiang, Q. Liu, Y. Lu, *Composites, Part B* **2023**, *254*, 110605.
[131] R. B. Ladani, M. Bhasin, S. Wu, A. R. Ravindran, K. Ghorbani, J. Zhang, A. J. Kinloch, A. P. Mouritz, C. H. Wang, *Eng. Fract. Mech.* **2018**, *203*, 102.
[132] A. R. Ravindran, R. B. Ladani, A. J. Kinloch, C.-H. Wang, A. P. Mouritz, *Compo., Part A* **2021**, *150*, 106624.
[133] G. Pappas, J. Botsis, *Int. J. Solids Struct.* **2016**, *85-86*, 114.
[134] L. P. Canal, M. Alfano, J. Botsis, *Compos. Sci. Technol.* **2017**, *139*, 90.
[135] S. P. Sharma, S. C. Lakkad, *Mater. Today Commun.* **2020**, *24*, 101016.
[136] J. Blanco, E. GarcÁa, R. Guzmán de Villoria, B. Wardle, *J. Compos. Mater.* **2009**, *43*, 825.
[137] Q. Peng, X. He, Y. Li, et al., *J. Mater. Chem.* **2012**, *22*, 5928.
[138] Q. Wu, H. Bai, A. Gao, J. Zhu, *Compos. Sci. Technol.* **2022**, *225*, 109522.
[139] Z. Jiang, X. Li, T. Zhang, et al., *Polymers* **2023**, *15*, 2147.
[140] R. Khan, *Compos. Struct.* **2019**, *229*, 111418.
[141] P. Hu, D. Pulungan, R. Tao, G. Lubineau, *Composites, Part A* **2021**, *149*, 106564.
[142] C. Hunt, J. Kratz, I. Partridge, *Composites, Part A* **2016**, *87*, 109.
[143] P. Prombut, L. Michel, F. Lachaud, J. Barrau, *Eng. Fract. Mech.* **2006**, *73*, 2427.
[144] P. Hu, D. Pulungan, R. Tao, G. Lubineau, *Composites, Part A* **2020**, *131*, 105783.
[145] M. De Moura, A. Pereira, A. De Morais, *Fatigue Fract. Eng. Mater. Struct.* **2004**, *27*, 759.
[146] M. Bin Mohamed Rehan, J. Rousseau, S. Fontaine, X. Gong, *Compos. Struct.* **2017**, *161*, 1.
[147] P. Hu, X. Li, G. Lubineau, *Compos. Sci. Technol.* **2023**, *233*, 109911.
[148] Y. Gong, L. Zhao, J. Zhang, Y. Wang, N. Hu, *Compos. Sci. Technol.* **2017**, *151*, 302.
[149] W. Xu, S. Zhang, W. Liu, Y. Yu, *Theor. Appl. Fract. Mech.* **2023**, *124*, 103734.
[150] J. Pascoe, S. Pimenta, S. Pinho, *Compos. Struct.* **2020**, *238*, 111932.
[151] Y. Ou, A. Fu, L. Wu, X. Yi, D. Mao, *Compos., Part A* **2024**, *176*, 107872.
[152] R. Tao, M. Alfano, G. Lubineau, *Compos., Part A* **2019**, *116*, 216.
[153] R. Tao, X. Li, A. Yudhanto, M. Alfano, G. Lubineau, *Compos., Part A* **2020**, *139*, 106094.
[154] K. Maloney, N. Fleck, *Int. J. Solids Struct.* **2019**, *158*, 66.
[155] C. Makabe, A. Murdani, K. Kuniyoshi, Y. Irei, A. Saimoto, *Eng. Fail. Anal.* **2009**, *16*, 475.
[156] A. Murdani, C. Makabe, A. Saimoto, Y. Irei, T. Miyazaki, *Eng. Fail. Ana.* **2008**, *15*, 810.
[157] A. Wagih, R. Tao, G. Lubineau, *Compos., Part A* **2021**, *149*, 106530.
[158] A. Wagih, G. Lubineau, *Compos. Sci. Technol.* **2021**, *204*, 108605.
[159] S. Hashemi, A. J. Kinloch, J. Williams, *Proceedings of the Royal Society of London. A. Mathematical and Physical Sciences* **1990**, *427*, 173.

[160] M. Kanninen, *Int. J. Fract.* **1974**, *10*, 415.
[161] J. Williams, *Compos. Sci. Technol.* **1989**, *35*, 367.
[162] A. Wagih, R. Tao, A. Yudhanto, G. Lubineau, *Compos., Part A* **2020**, *134*, 105892.
[163] R. Fernandes, J. Chousal, M. De Moura, J. Xavier, *Compos., Part B* **2013**, *52*, 269.
[164] T. Löbel, D. Holzhüter, M. Sinapius, C. Hühne, *Int. J. Adhes. Adhes.* **2016**, *68*, 229.
[165] R. Garcia, P. Prabhakar, *Compos. Struct.* **2017**, *176*, 547.
[166] S. Heide-Jørgensen, S. Teixeira de Freitas, M. K. Budzik, *Compos. Sci. Technol.* **2018**, *160*, 97.
[167] M. Pawlik, L. Y. Yu Cheah, U. Gunputh, H. Le, P. Wood, Y. Lu, *Int. J. Adhes. Adhes.* **2022**, *114*, 103105.
[168] R. Ritchie, *Nat. Mater.* **2011**, *10*, 817.
[169] D. Davis, B. Whelan, *Composites: Part B* **2011**, *42*, 105.
[170] S. Joshi, V. Dikshit, *J. Compos. Mater.* **2012**, *46*, 665.
[171] F. Mujika, G. Vargas, J. Ibarretxe, J. DeGracia, A. Arrese, *Composites: Part B* **2012**, *43*, 1336.
[172] K. Almuhammadi, M. Alfano, Y. Yang, G. Lubineau, *Mater. Design* **2014**, *53*, 921.
[173] K. Maloney, N. Fleck, *Int. J. Solids Struct.* **2019**, *158*, 66.
[174] M. Alfano, C. Morano, L. Bruno, M. Muzzupappa, L. Pagnotta, in *Procedia Structural Integrity*, vol. *8*, **2018**, 604–609.
[175] S. Xia, L. Ponson, G. Ravichandran, K. Bhattacharya, *Phys. Rev. Lett.* **2012**, *108*.
[176] S. Xia, L. Ponson, G. Ravichandran, K. Bhattacharya, *J. Mech. Phys. Solids* **2013**, *61*, 838.
[177] C. Morano, P. Zavattieri, M. Alfano, *J. Mech. Phys. Solids* **2020**, *141*, 103965.
[178] A. Luo, K. T. Turner, *J. Mech. Phys. Solids* **2022**, *159*, 104713.
[179] T. Pardoen, K. Turner, M. Budzik, *Advances in Structural Adhesive Bonding*, second edition Edition, **2023**, pp. 1105–1122.
[180] C. Morano, M. Scagliola, L. Bruno, M. Alfano, *Int. J. Adhes. Adhes.* **2024**, *131*, 103660.
[181] K. Kendall, *Proceedings of the Royal Society of London. Series A. Mathematical and Physical Sciences* **1975**, *341*, 409.
[182] C.-J. Hsueh, L. Avellar, B. Bourdin, G. Ravichandran, K. Bhattacharya, *J. Mech. Phys. Solids* **2018**, *120*, 68.
[183] N. Wang, S. Xia, *J. Mech. Phys. Solids* **2017**, *98*, 87.
[184] C. Morano, N. Terasaki, T. Gao, G. Lubineau, M. Alfano, *ACS Appl. Mater. Interf.* **2023**, *15*, 40887.
[185] C. Morano, R. Tao, A. Wagih, M. Alfano, G. Lubineau, *Mater. Today Commun.* **2022**, *32*, 104103.
[186] A. Afshar, A. Daneshyar, S. Mohammadi, *Compos. Struct.* **2015**, *125*, 314.
[187] S. M. Jensen, M. Martos, B. L. V. Bak, E. Lindgaard, *Compos. Struct.* **2019**, *216*, 477.
[188] Y. Gong, Y. Hou, L. Zhao, W. Li, J. Zhang, N. Hu, *Int. J. Mech. Sci.* **2020**, *176*, 105514.
[189] S. Abdel-Monsef, B. Tijs, J. Renart, A. Turon, *Eng. Fract. Mech.* **2023**, *284*, 109233.
[190] G. A. Pappas, J. Botsis, *Compos. Sci. Technol.* **2020**, *197*, 108172.
[191] P. Lagace, J. Brewer, C. Kassapoglou, *Compos. Technol. Res.* **1987**, *9*, 81.
[192] C. Wang, X. Xu, *Compos. Struct.* **2015**, *134*, 176.
[193] M. Beghini, L. Bertini, P. Forte, *Compos. Sci. Technol.* **2006**, *66*, 240.
[194] T. Sebaey, N. Blanco, C. Lopes, J. Costa, *Compos. Sci. Technol.* **2011**, *71*, 1587.
[195] J. Andersons, M. König, *Compos. Sci. Technol.* **2004**, *64*, 2139.
[196] E. Triki, B. Zouari, F. Dammak, *Eng. Fract. Mech.* **2016**, *159*, 63.
[197] H. Albertsen, J. Ivens, P. Peters, M. Wevers, I. Verpoest, *Compos. Sci. Technol.* **1995**, *54*, 133.
[198] X. Li, B. van der Heijden, P. Hu, H. Eddine Rekik, G. Lubineau, *Composites, Part B* **2024**, Submitted.
[199] L. Carreras, B. Bak, A. Turon, J. Renart, E. Lindgaard, *European Journal of Mechanics-A/Solids* **2018**, *72*, 464.
[200] Z. R. Khokhar, I. A. Ashcroft, V. V. Silberschmidt, *Comput. Mater. Sci.* **2009**, *46*, 607.
[201] I. Ashcroft, Z. Khokar, V. Silberschmidt, *Comput. Mater. Sci.* **2012**, *52*, 95.
[202] L. Canal, G. Pappas, J. Botsis, *Compos. Sci. Technol.* **2016**, *126*, 52.
[203] D. Pulungan, S. Andika, T. Dirgantara, R. Wirawan, H. Judawisastra, S. Wicaksono, *Composites, Part A* **2024**, 108107.
[204] R. Rafiee, M. Sahraei, *Compos. Sci. Technol.* **2021**, *201*, 108487.
[205] F. Daghia, V. Fouquet, L. Mabileau, *Int. J. Solids Struct.* **2022**, *254*, 111910.
[206] W. Xu, H. Yu, C. Tao, *Int. J. Adhes. Adhes.* **2014**, *52*, 48.
[207] R. Sills, M. Thouless, *Int. J. Solids Struct.* **2015**, *55*, 32.
[208] C. P. Puspaningtyas, A. Jusuf, B. K. Hadi, A. Yudhanto, *Heliyon* **2024**, *10*, 2.
[209] X. Li, R. Tao, M. Alfano, G. Lubineau, *Int. J. Solids Struct.* **2020**, *191*, 87.
[210] X. Li, R. Tao, A. Yudhanto, G. Lubineau, *Int. J. Solids Struct.* **2020**, *196*, 41.
[211] M. Herráez, N. Pichler, J. Botsis, *Compos. Struct.* **2020**, *247*, 112422.
[212] X. Li, S. Lu, G. Lubineau, *Int. J. Solids Struct.* **2021**, *233*, 111150.
[213] Z. Czech, R. Milker, *Mater. Sci.* **2005**, *23*, 4.
[214] S. B. Lin, L. D. Durfee, R. A. Ekeland, J. McVie, G. K. Schalau, *J. Adhes. Sci. Technol.* **2007**, *21*, 605.
[215] S. Mapari, S. Mestry, S. Mhaske, *Polym. Bull.* **2021**, *78*, 4075.
[216] F. Matthews, P. Kilty, E. Godwin, *Composites* **1982**, *13*, 29.
[217] A. Wagih, F. Oz, G. Lubineau, *J. Mater. Res. Technol.* **2024**, *28*, 255.
[218] A. Wagih, H. A. Mahmoud, R. Tao, G. Lubineau, *Polymers* **2023**, *15*, 259.
[219] Z. Li, A. Haigh, C. Soutis, A. Gibson, R. Sloan, N. Karimian, *Adv. Compos. Lett.* **2016**, *25*, 83.
[220] M. Thawre, K. Pandey, A. Dubey, K. Verma, D. Peshwe, R. Paretkar, N. Jagannathan, C. Manjunatha, *Compos. Struct.* **2015**, *127*, 260.
[221] E. Greenhalgh, M. Hiley, *Composites, Part A* **2003**, *34*, 151.
[222] M. Hashem, A. Wagih, G. Lubineau, *Compos. Struct.* **2022**, *291*, 115545.
[223] S. Hisada, S. Minakuchi, N. Takeda, *Compos. Struct.* **2020**, *253*, 112792.
[224] A. R. Ravindran, R. Ladani, C. Wang, A. Mouritz, *Compos. Struct.* **2020**, *255*.
[225] L. A. Burns, A. P. Mouritz, D. A. Pook, S. Feih, *Compos. Part B-engineering* **2015**, *69*, 222.
[226] A. Wagih, M. Hashem, G. Lubineau, *Compos. Part A* **2022**, *162*, 107134.
[227] C. Morano, A. Wagih, M. Alfano, G. Lubineau, *Compos. Struct.* **2023**, *307*, 116652.
[228] A. Wagih, H. A. Mahmoud, G. Lubineau, *Mater. Des.* **2024**, 112963.

Gilles Lubineau is professor of Mechanical Engineering in the Physical Science and Engineering Division at KAUST, leading the MCEM Lab and Director of ENERCOMP, a Technology Consortium for Composites in Energy. Following his "aggregation" in theoretical mechanics, Pr. Lubineau earned a PhD from École Normale Supérieure Cachan, France. He was a faculty member at ENS-Cachan, and Instructor at École Polytechnique. He served as a visiting researcher at UC-Berkeley and as Interim Dean of the PSE Division at KAUST. His research covers: integrity of composite materials and structures, inverse problems for the identification of constitutive parameters, multi-scale techniques, multifunctional materials.

Marco Alfano holds a Laurea in Mechanical Engineering and a Ph.D. in Materials and Structures Engineering from the University of Calabria (UNICAL). He completed post-doctoral fellowships at UNICAL, the University of Illinois (Fulbright Scholar), and KAUST. Prof. Alfano subsequently assumed faculty positions at UNICAL (assistant professor) and the University of Waterloo (associate professor). He is currently Full Professor at the University of Modena and Reggio Emilia and serves as an Adjunct Professor at Waterloo. His research focuses on the fracture of polymers, adhesives, and composites, with particular emphasis on the mechanics of interfaces and adhesion.

Dr. Ran Tao is a postdoc researcher in Aerospace Structures & Materials in Faculty of Aerospace Engineering at TU Delft. Dr. Tao earned a PhD from the PSE Division at KAUST under the supervision of Pr. Gilles Lubineau. His research covers: mode I fracture of adhesively bonded composite joints, numerical modelling of structure failure using cohesive zone model, X-ray computed tomography assisted microstructure characterization.

Ahmed Wagih is a research scientist in Mechanics of Composites for Energy and Mobility lab (MCEM) at KAUST and track leader for composite performance in ENERCOMP, a Technology Consortium for Composites in Energy. Dr. Wagih earned his MS and PhD degrees from Girona University, Spain. After that, he was a faculty member at Zagazig University, Egypt. Before Joining KAUST, he served as a postdoc researcher at Chalmers University, Sweden. His research covers: Toughening of composite structures, integrity of composite materials and structures, and testing in harsh environment.

Arief Yudhanto is a research scientist at the Department of Mechanical Engineering, Baylor University, Waco, TX, USA. He used to work as a research scientist at the Composites Lab. of KAUST, an assistant research professor at Tokyo Metropolitan University, and engineer at Hitachi GST and A*STAR Singapore. He has been working in composite materials (adhesive bonding, additive manufacturing, thermoplastics, 3D composites, damage mechanics, failure theory). He earned BS in aerospace engineering from Institut Teknologi Bandung, MS in mechanical engineering from National University of Singapore, and PhD in aerospace engineering from Tokyo Metropolitan University.

Xiaole Li is a research scientist from Mechanical Engineering in the Physical Science and Engineering Division at KAUST, acting as the track leader on digital modeling in ENERCOMP, a Technology Consortium for Composites in Energy. He holds a PhD in civil engineering from the University of the Portsmouth, UK. His research interests include: Fracture mechanics of composite structures, Mechanics of soft interfaces, Predictive models for composites.

Mjed Hashem a Senior Materials Specialist at NEOM's Design and Construction sector, leads projects to innovate materials engineering and construction practices. With a BSc. (Hons) in Materials Science and Engineering from the University of Manchester and an MSc. from KAUST, Mjed seamlessly merges academic and industry expertise. His research on enhancing energy dissipation in CFRP T-joint structures showcases dedication to materials engineering advancement. Having garnered experience at esteemed organizations like KFUPM and Saudi Aramco, Mjed now leads R&D initiatives at NEOM's Engineering Innovations Department. His zeal for composites drives ongoing innovation, aiming to bridge theory and application in materials science.

Khaled Almuhammadi is the Chief Technology Officer (CTO) at Novel Non-Metallic Solutions. He is leading the technology edge of the JV between Saudi Aramco and Baker Hughes towards delivering the vision and mission of the company. Almuhammadi has a mechanical engineering background along with master's and PhD degrees from KAUST specialized in composite materials with about two decades of professional working experience. His expertise covers diverse aspects in both upstream and downstream domains in Saudi Aramco, besides hands-on experience in conducting and managing scientific research projects for composites, as well as has published several scientific journal papers and patents.

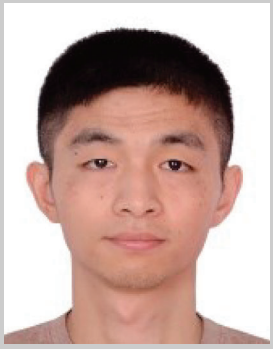

Ping Hu is a post-doc researcher in the Department of Mechanics and Production at Aarhus University. Dr. Hu earned a PhD in the Mechanical Engineering program from KAUST in the study of fracture mechanics of composite materials.

Hassan Mahmoud received the B.S. and M.S. degrees in Mechanical Engineering from Cairo University, Cairo, Egypt in 2017 and 2021 respectively. Currently, he is a PhD candidate in Mechanical Engineering in the Physical Science and Engineering Division at KAUST. His research covers: the design and fabrication of wireless sensors, printed electronics, structural health monitoring, and integrity of composite materials and structures.

Fatih Ertugrul Oz is a postdoctoral research fellow in the Mechanics of Composites for Energy and Mobility research group at KAUST and working as a researcher in ENERCOMP, a Technology Consortium for Composites in Energy. He attained his BSc in Manufacturing Engineering from Istanbul Technical University and pursued his MSc and PhD in Mechanical Engineering department at Bogazici University. He has a background as an assistant professor across multiple universities and industry experience in various engineering and R&D departments. His primary research interests are Damage Mechanics and Non-Destructive Testing (NDT) of composite materials and sandwich structures.